Respiratory Fluid Mechanics

J.B. Grotberg, Ph.D., M.D.
Department of Biomedical Engineering
University of Michigan

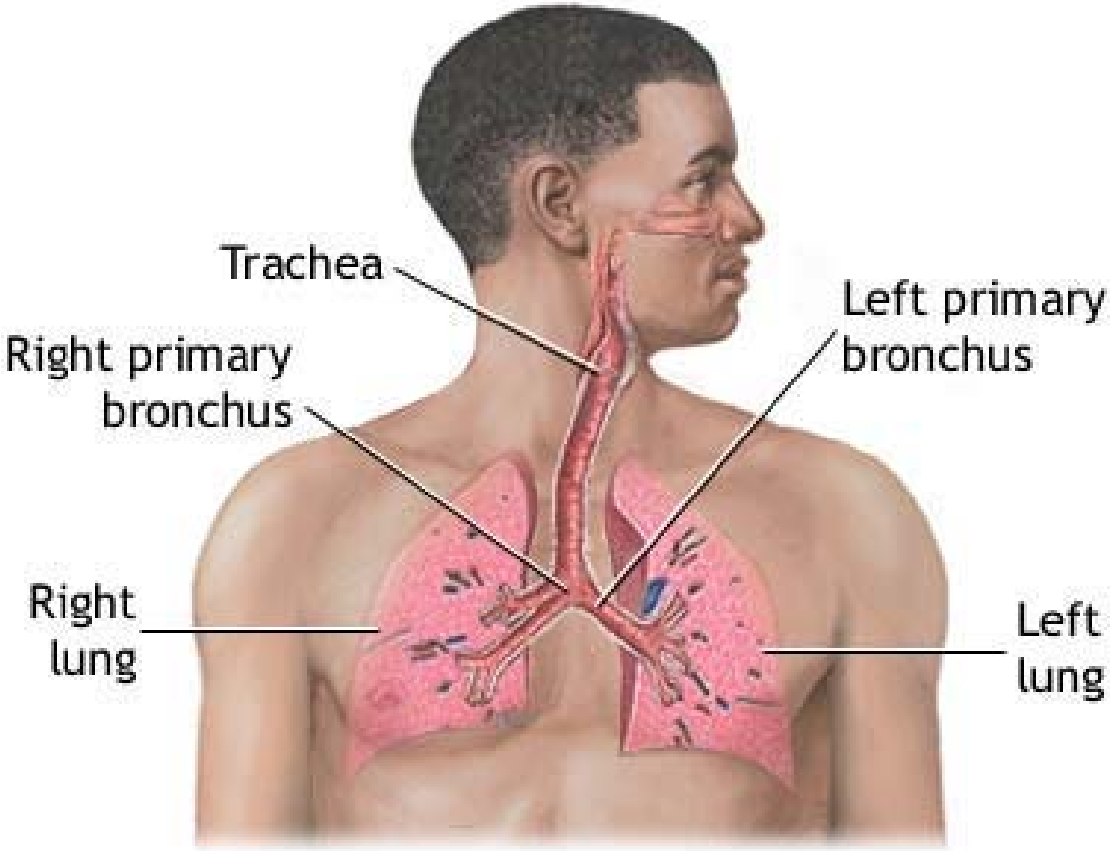

Airway Branching Network

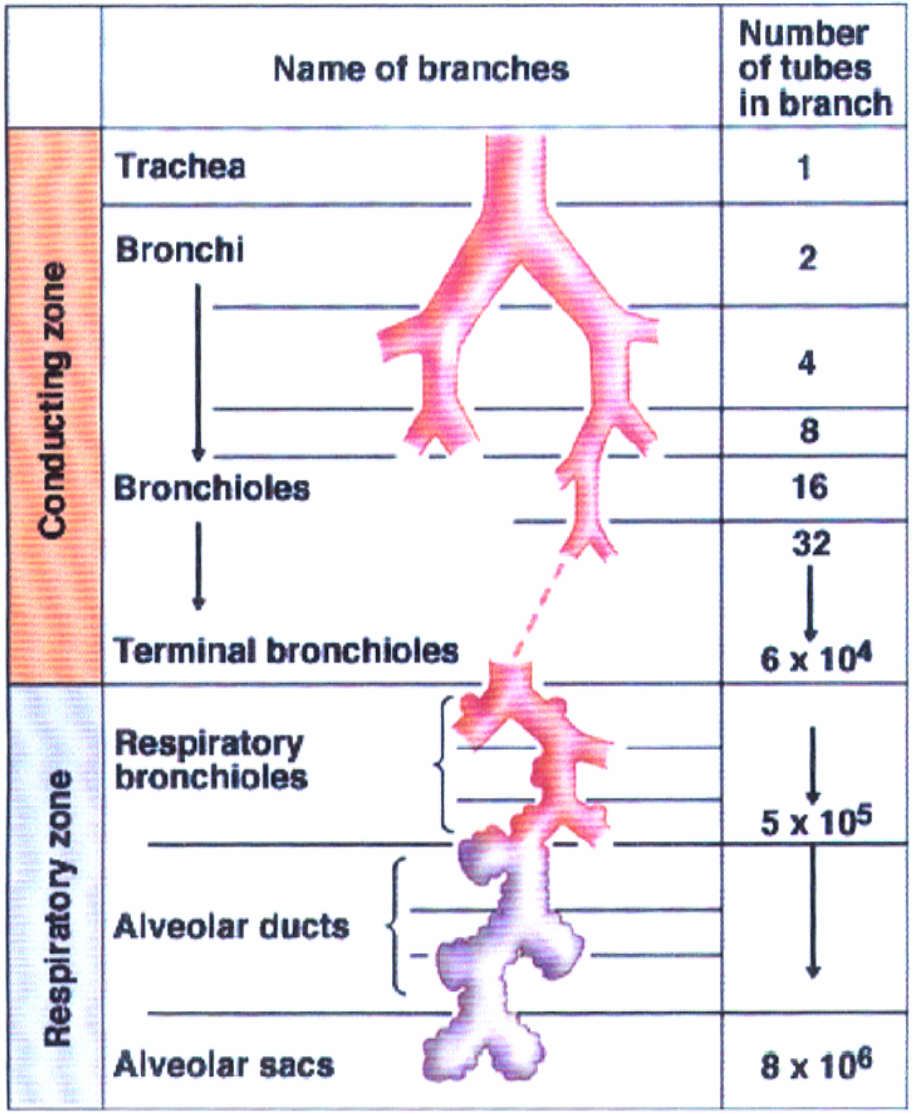

Respiratory Zone

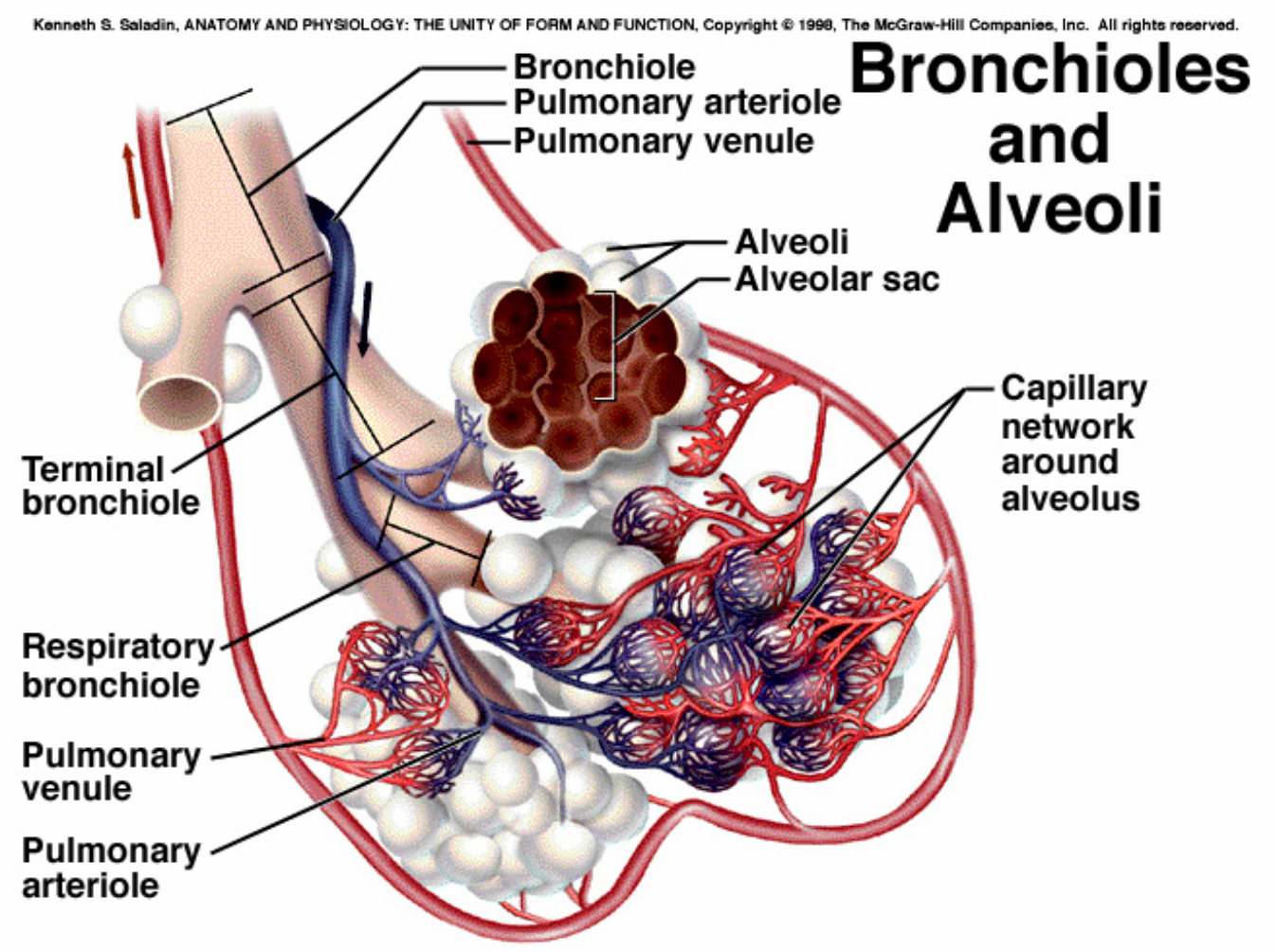

Airway and Alveolar Liquid Lining

Cultured human tracheo-bronchial airway epithelia

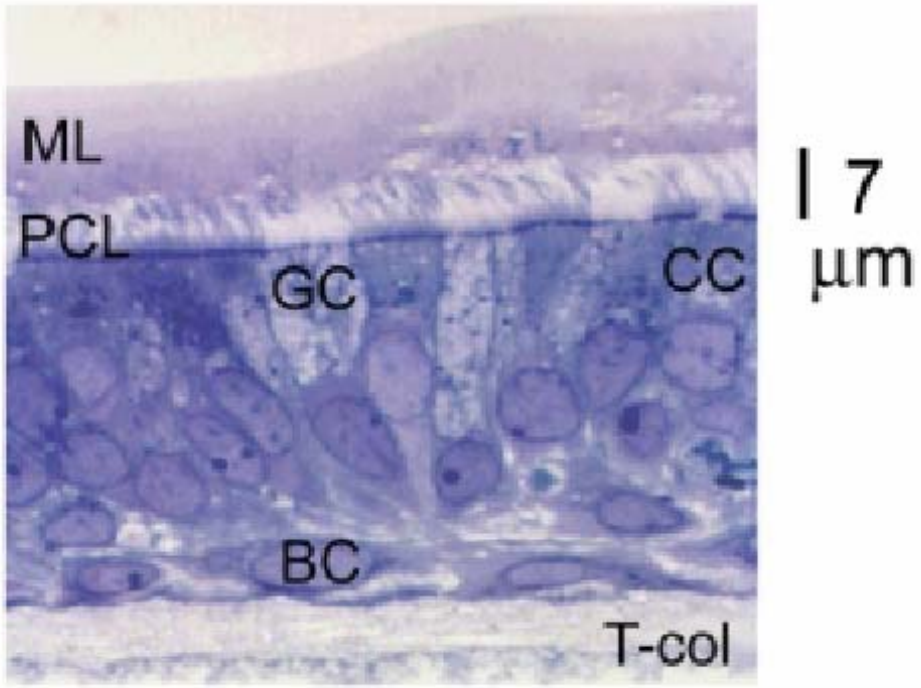

ML-mucus layer, PCL-periciliary layer, GC-goblet cell, CC-ciliated cell, BC-basal cell, T-col-semipermeable supports

Measurements of Airway Surface Liquid Height (Volume) by Confocal Microscopy

Authors: Robert Tarran and Brian Button

Cystic Fibrosis/Pulmonary Research and Treatment Center, The University of North Carolina at Chapel Hill, Chapel Hill, NC, USA

e-mail: robert_tarran@med.unc.edu, brian_button@med.unc.edu

Alveolar liquid lining and surfactant system

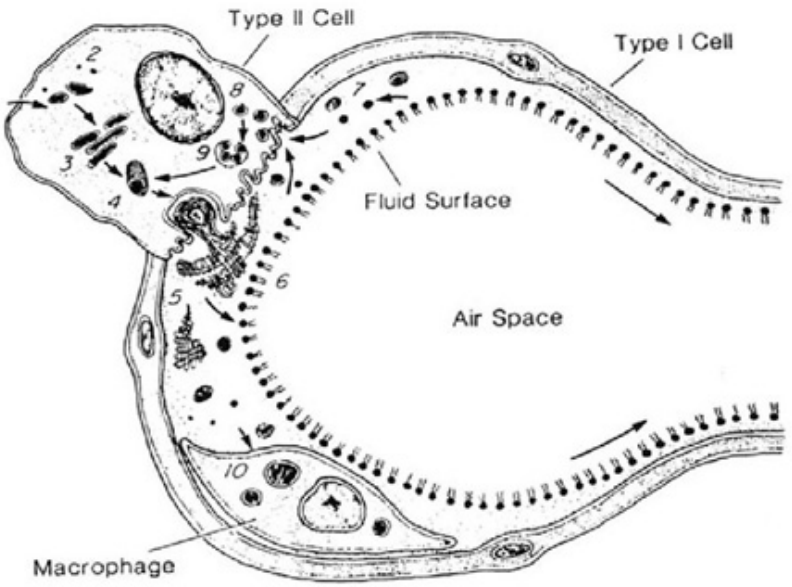

Airway Liquid Plugs: How Do They Occur?

- Intrinsic
  - Normal people at full expiration
  - Congestive Heart Failure $\rightarrow$ Pulmonary Edema
  - Asthma, Emphysema
- Extrinsic
  - Surfactant Replacement Therapy
  - Delivery of Drugs, Genetic Material, Stem Cells
  - Liquid Ventilation
  - Drowning

Example of Extrinsic Plug: Surfactant Replacement Therapy

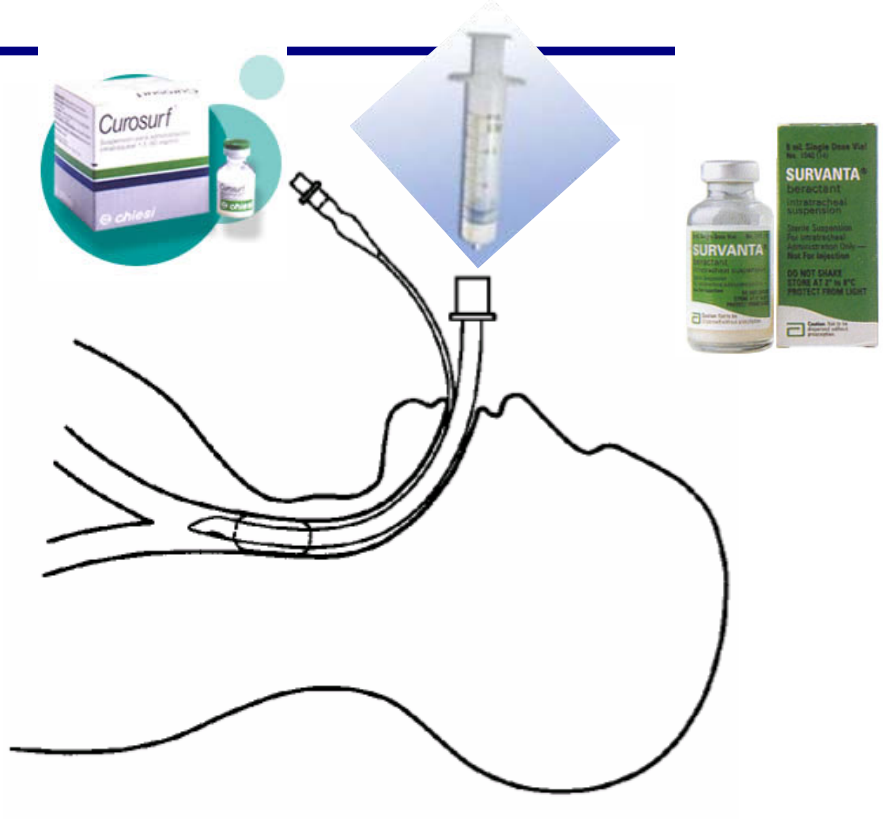

-- Surfactant replacement therapy in premature infants.
-- Partial or total liquid ventilation.
-- Drug and gene delivery.

Experimental Setup – Lung Close-up

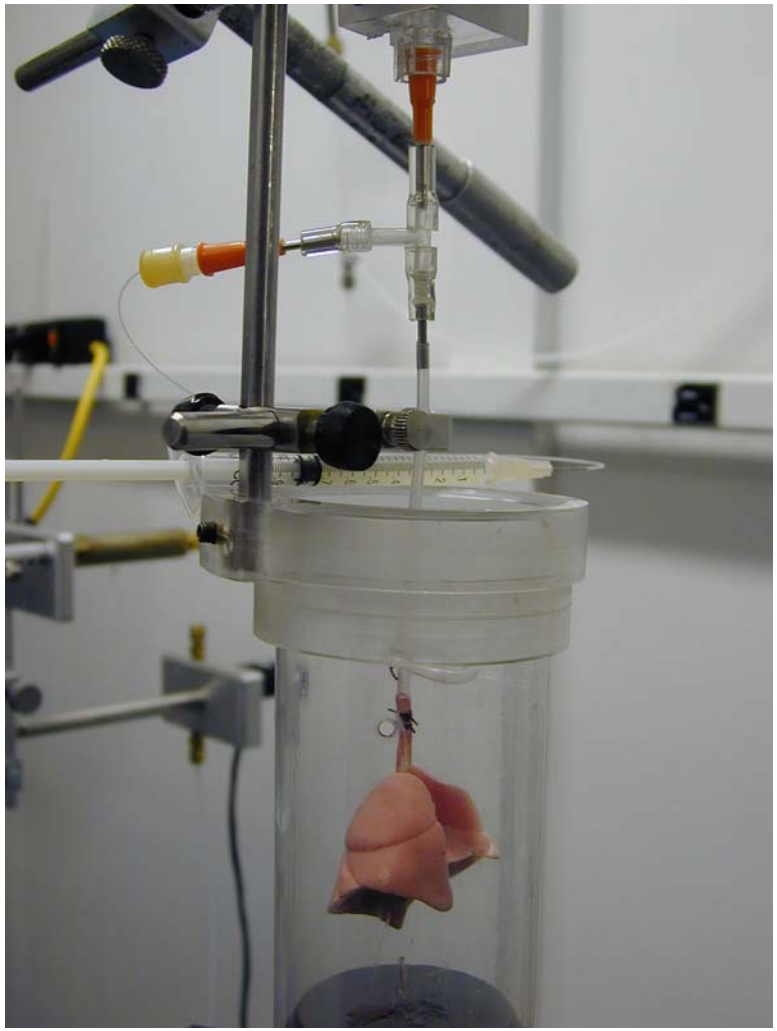

(Courtesy of Robert Mothen, Medical College of Wisconsin, Milwaukee, WI)

- **The excised lung suspended and ventilated from tracheal cannula.**
- **A small diameter tube attached to a syringe was inserted into the cannula (upper center of figure).**
- **A surfactant bolus was formed in the cannula by injecting 0.05 ml of surfactant through the small diameter tube.**

Cassidy, K.J., J.L. Bull, M.R. Glucksberg, C.A. Dawson, S.T. Haworth, R.B. Hirschl, N. Gavriely and J.B. Grotberg. J. Appl. Physiol. 2001.

Anderson, J.C., R.C. Molthen, C.A. Dawson, S.T. Haworth, J.L. Bull, M.R. Glucksberg and J.B. Grotberg. J. Appl. Physiol. 2004.

Micro-CT Movie of Surfactant Instillation – Single Dose

(Click image to start/stop movie)

Experimental Conditions

- **Excised Rat Lung**
- **Lung Suspended Vertically**
- **Normal Bolus Volume**
- **Surfactant = Survanta**
- **Ventilation Rate - 60 br/min**

Example of Intrinsic Plug: Airway Closure

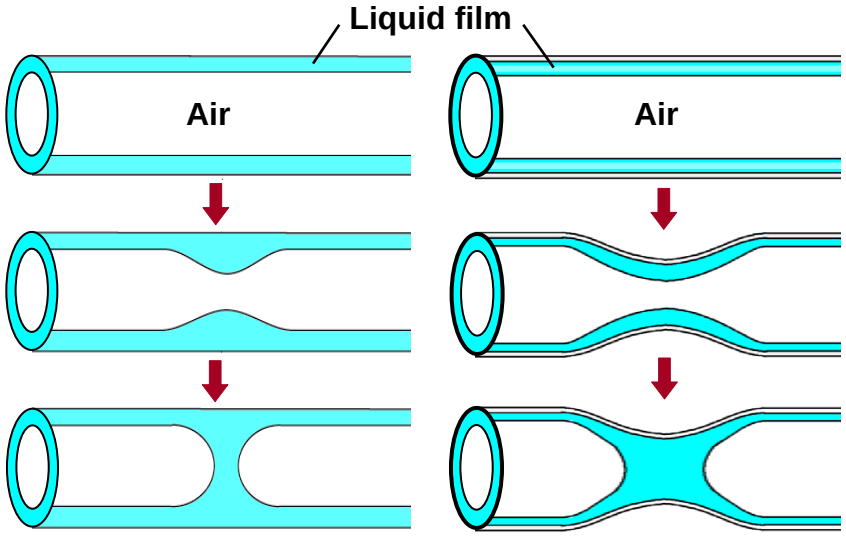

Airway closure Instability & plug formation

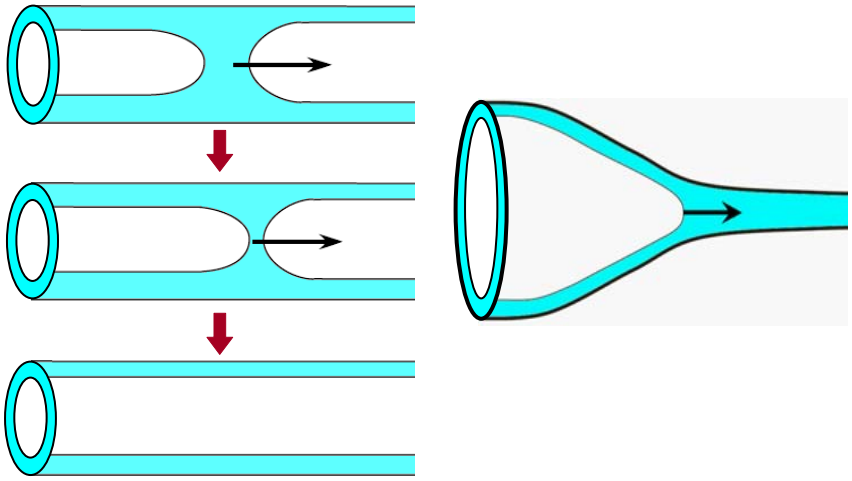

Airway reopening plug propagation & rupture

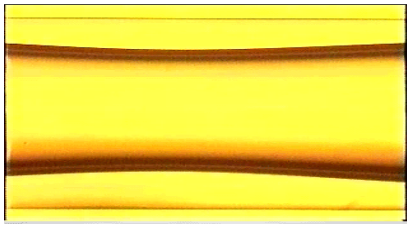

Cassidy et al., *J. Appl. Physiol.* **1999**

Asymptotic Approach to Liquid Plug Propagation

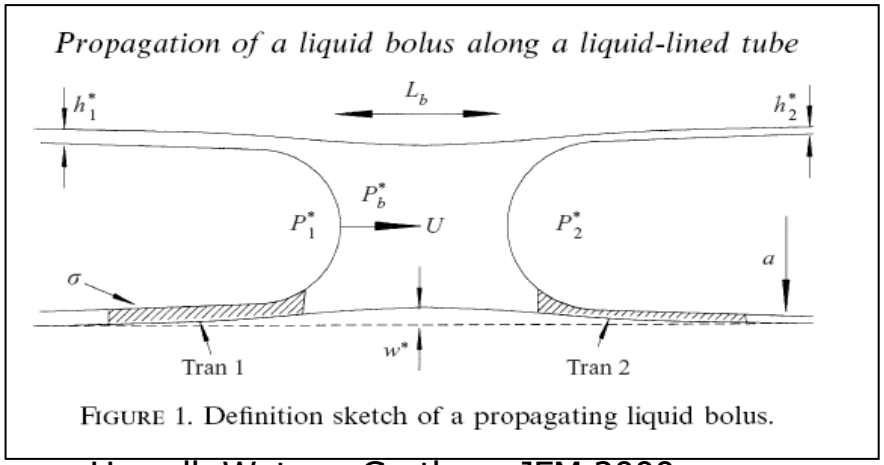

FIGURE 1. Definition sketch of a propagating liquid bolus.

Howell, Waters, Grotberg JFM 2000

Re=0, $Ca^{1/3}$<<1, wall elastance & tension

Plug core viscous effects O(Ca), negligible

Transition regions dominate, $G_1 \to 0$ rigid

$$\eta_{\zeta\zeta\zeta} = \frac{\eta - G_1\eta_{\zeta\zeta} - 1}{(\eta - G_1\eta_{\zeta\zeta})^3}.$$

Generalized Landau-Levich Eq

Outer, inner, intermediate regions

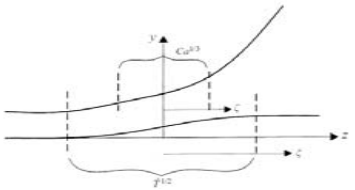

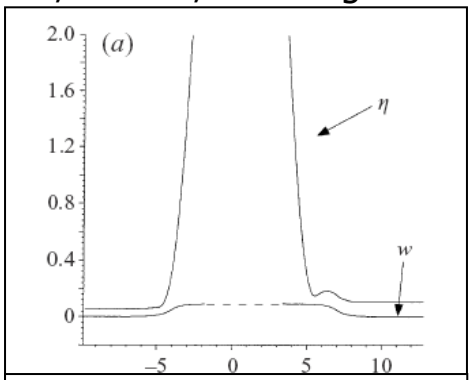

h_2 (input) vs h_1 (output)

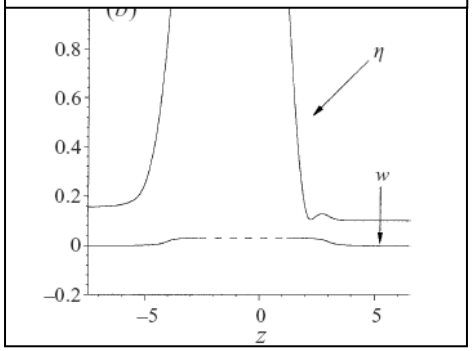

$$\frac{d(Vol_{plug})}{dt}$$

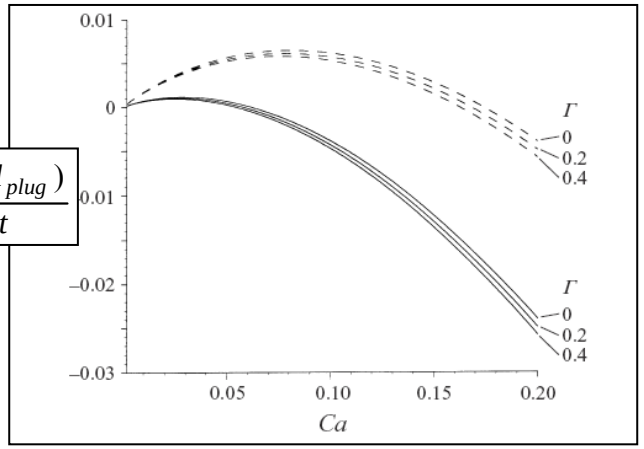

Plug Rupture Criteria:
Airway Reopening $h_1 > h_2$

2-D Steady Plug Propagation in Channel

Fujioka, Grotberg PoF 2005

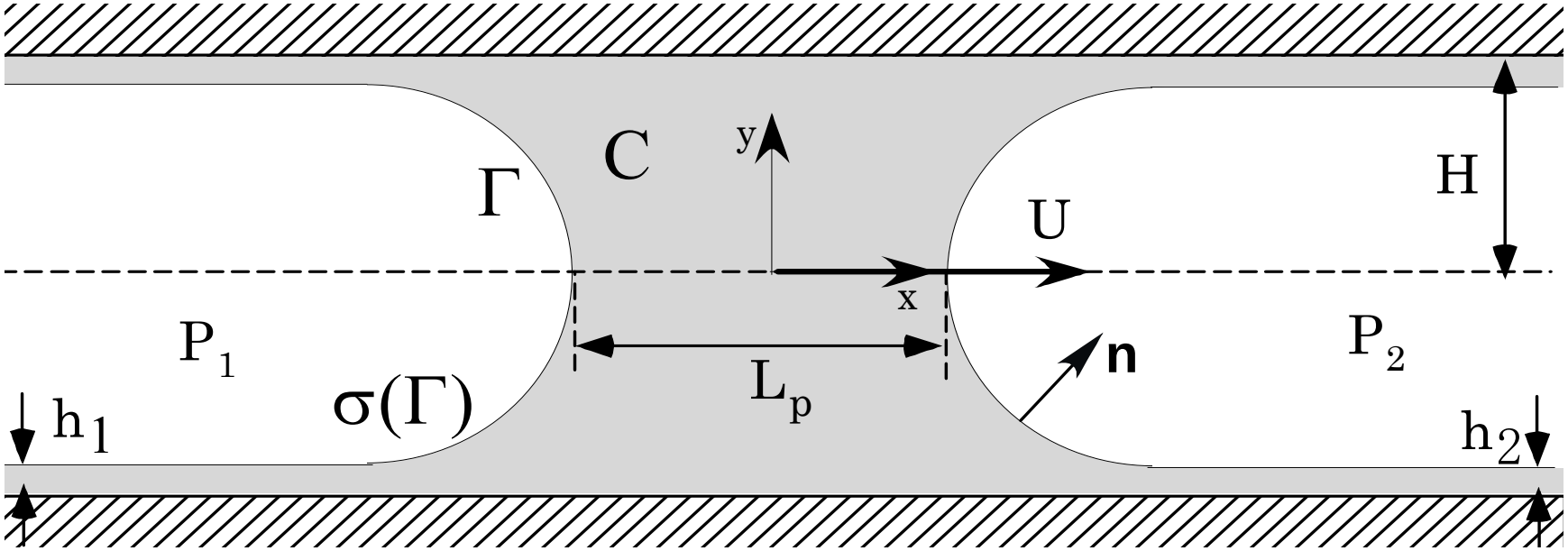

- $\Delta P=P_1-P_2$ drives plug at constant speed U.
- $h_2=h_1$, for the steady state.
- Soluble surfactant, Newtonian fluid.
- Surfactant in far precursor film is prescribed.
- L_p/H, $h_2/H=h_1/H$ prescribed for steady state.

Flow Governing Equations

- Scaling with $p = p^* / \frac{\mu U}{H},\ \mathbf{u} = \mathbf{u}^* / U,\ \mathbf{x} = \mathbf{x}^* / H$
- Dimensionless Navier-Stokes and the continuity equations.

$$\mathrm{Re}\left(\mathbf{u}\cdot\nabla\right)\mathbf{u} = -\nabla p + \nabla^2\mathbf{u} \qquad \nabla\cdot\mathbf{u} = 0$$

- Boundary condition along free interface.

$$-p\mathbf{n} + \left(\nabla\mathbf{u} + \nabla\mathbf{u}^T\right)\cdot\mathbf{n} = Ca^{-1}\left(\sigma\kappa\mathbf{n} + \nabla_s\sigma\right) - P_a\mathbf{n} \qquad \mathbf{u}\cdot\mathbf{n} = 0$$

$\mathbf{n}$ Normal vector on interface κ Curvature of interface

σ_M Surface tension in surfactant-free interface

- Dimensionless Parameters

$$\mathrm{Re} = \frac{\rho HU}{\mu}, Ca = \frac{\mu U}{\sigma_M} \quad or \quad \mathrm{Re} = \frac{\rho HU}{\mu}, \lambda = \frac{\mathrm{Re}}{Ca} = \frac{\rho\sigma_M H}{\mu^2}$$

Surfactant Transport Equations

- Scaling with $C = C^* / C^*_{cmc},\ \Gamma = \Gamma^* / \Gamma^*_{\infty}$

- Bulk surfactant transport equations.

$$Sc\,\mathrm{Re}\,\nabla\cdot\left(\mathbf{u}C\right) = \nabla^2 C \qquad \text{BC } -\frac{Sc_s}{\chi Sc}\left(\mathbf{n}\cdot\nabla\right)C = j_n$$

- Interfacial surfactant transport equations.

$$Sc_s\,\mathrm{Re}\,\nabla_s\cdot\left(\mathbf{u}\Gamma\right) - \nabla_s{}^2\Gamma = j_n$$

- Dimensionless Parameters, $Sc = \frac{\mu}{\rho D},\ Sc_s = \frac{\mu}{\rho D_s},\ \chi = \frac{\Gamma_\infty{}^*}{C_{cmc}{}^* H}$

Γ^*_{∞} Maximum monolayer packing value of Γ^*

C^*_{cmc} Critical Micelle Concentration

Surfactant Transport Equations (2)

- Surfactant flux from the bulk to the interface

$$j_n = \begin{cases} K_a C_s \left(1-\Gamma\right) - K_d \Gamma & \left(\Gamma < 1\right) \\ -K_d \Gamma & \left(\Gamma \geq 1\right) \end{cases}$$

- Modified Frumkin equation of state

$$\sigma = \begin{cases} 1 - E\Gamma & \left(\Gamma < 1\right) \\ \left(1-E\right)\exp\left[\dfrac{E}{1-E}\left(1-\Gamma\right)\right] & \left(\Gamma \geq 1\right) \end{cases}$$

- Dimensionless Parameters, $K_a = \dfrac{k_a C^*_{cmc} H^2}{D_s}$, $K_d = \dfrac{k_d H^2}{D_s}$, $E = -\dfrac{\Gamma^*_\infty}{\sigma^*_M}\dfrac{\partial \sigma^*}{\partial \Gamma^*}$

k_a Adsorption rate coefficient
k_d Desorption rate coefficient
C_s Bulk surfactant concentration in subsurface

Flow and Pressure: No Surfactant

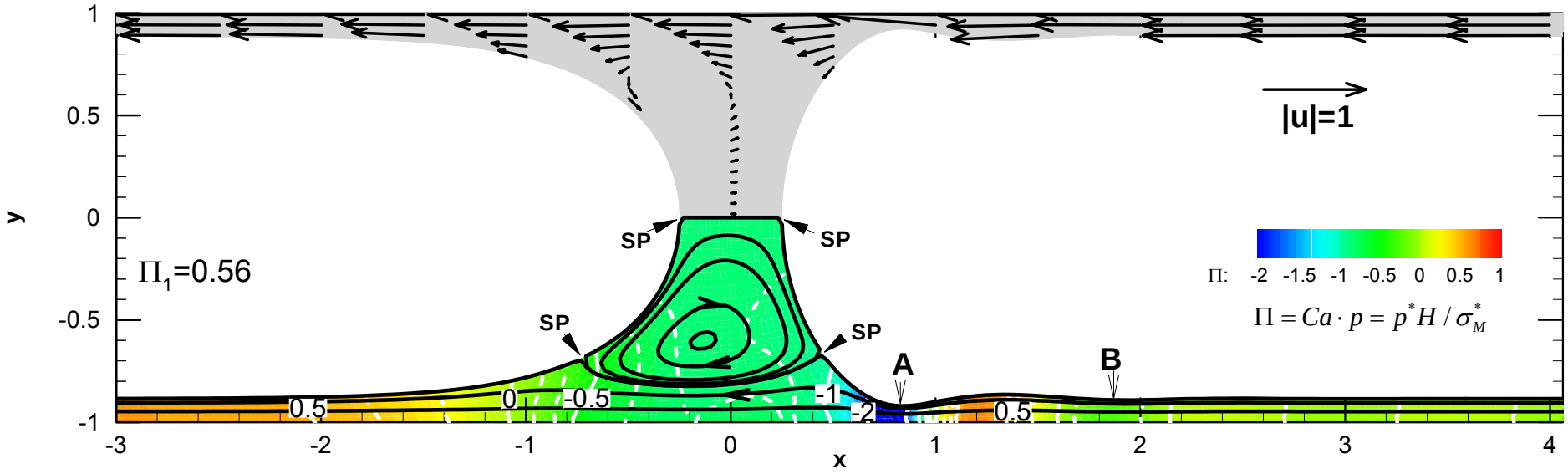

Re=50, λ=1000, L_P=0.5

- 4 stagnation points in the half-domain, all on the interface.
- Two flow regions: recirculation and flow-through
- Recirculation region low velocity
- Capillary wave at front
- Pressure minimized at A (in capillary wave)

Flow, Pressure, and Surfactant (Lp=0.5)

Re=50,λ=1000, L_P=0.5, Sc=10, Sc_s=100,
$K_a=10^4$, $K_b=10^2$, $\chi=10^{-3}$, E=0.7, $C_0=10^{-4}$

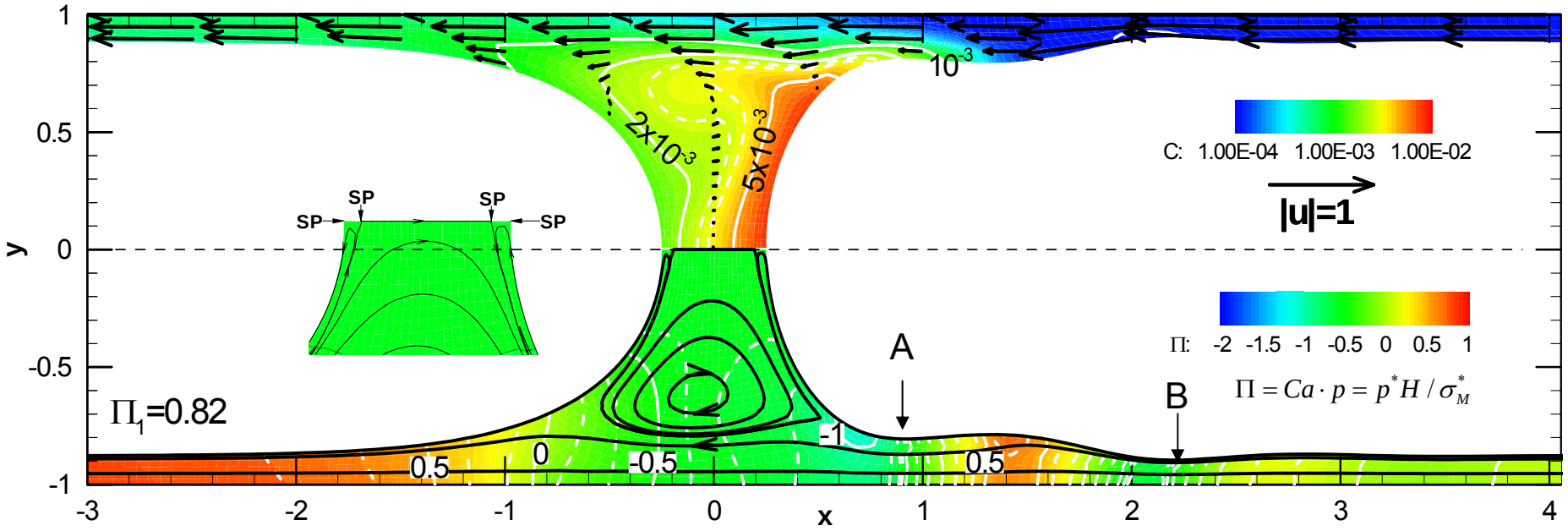

- 4 stagnation points on midline, 2 on interface, 2 internal
- The recirculation zone is no longer in contact with the interfaces.
- Thicker transition region at front, thinnest point at B
- The maximum concentration attains at the front meniscus

Flow, Pressure, and Surfactant (Lp=2.0)

Re=50,λ=1000, L_P=2, Sc=10, Sc_s=100,
$K_a=10^4$, $K_b=10^2$, $\chi=10^{-3}$, E=0.7, $C_0=10^{-4}$

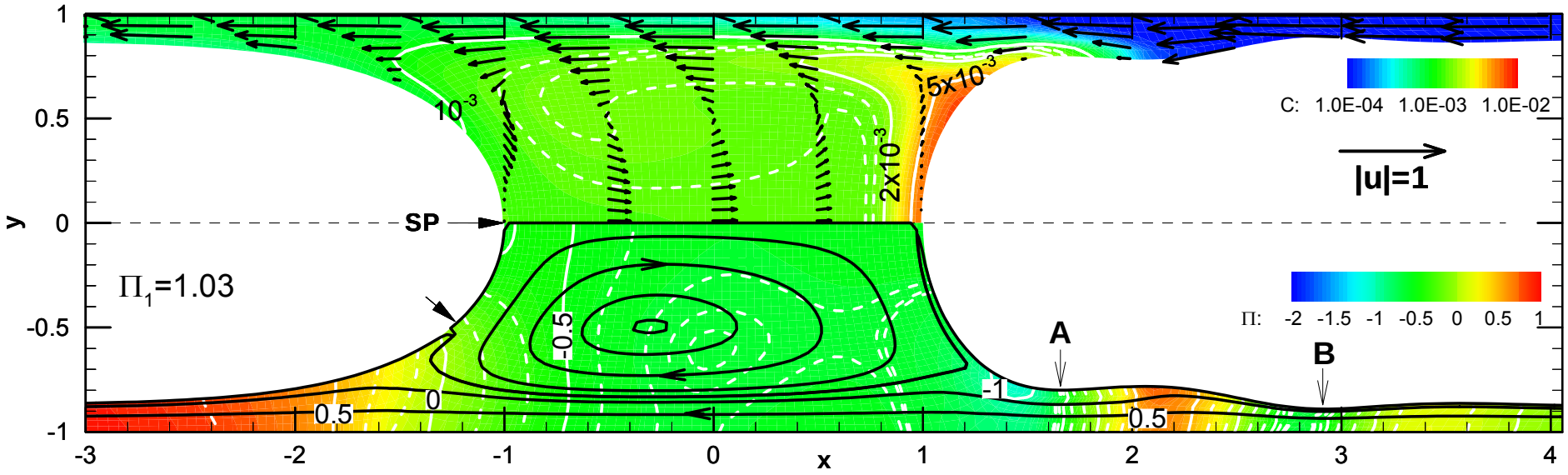

- Front meniscus stagnation pts. differ from rear.
- Velocity profiles fully developed at the middle cross-section ~ parabolic.
- Concentric iso-pressure lines appear due to centrifugal forces.

Wall Pressure and Shear Stress

λ=1000, L_P=2, Sc=10, Sc_s=100, $K_a=10^4$,
$K_b=10^2$, $\chi=10^{-3}$, E=0.7, $C_0=10^{-4}$

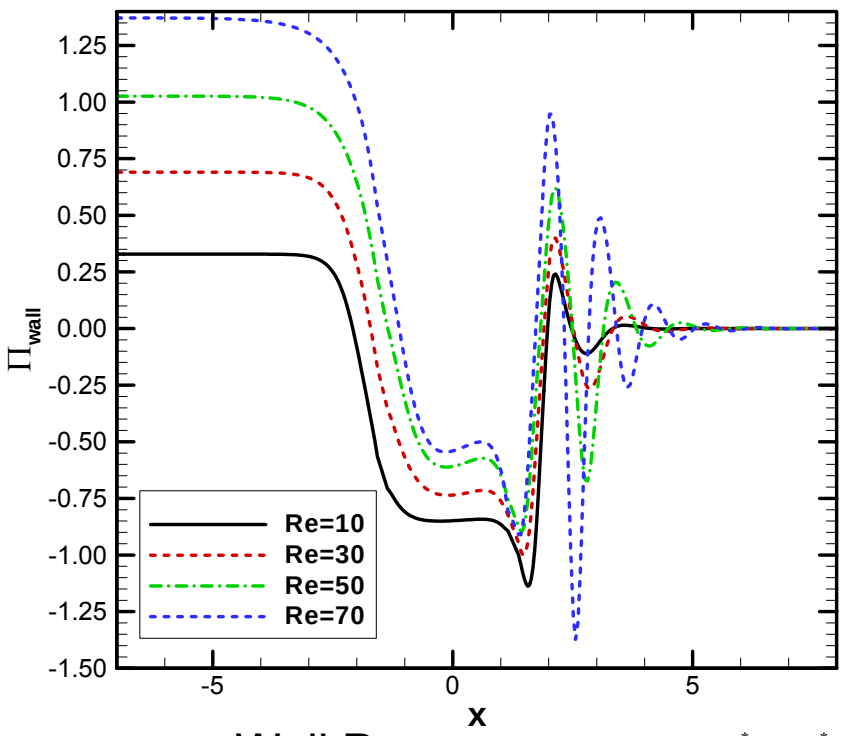

Wall Pressure $\Pi = Ca \cdot p = p^* H / \sigma_M^*$

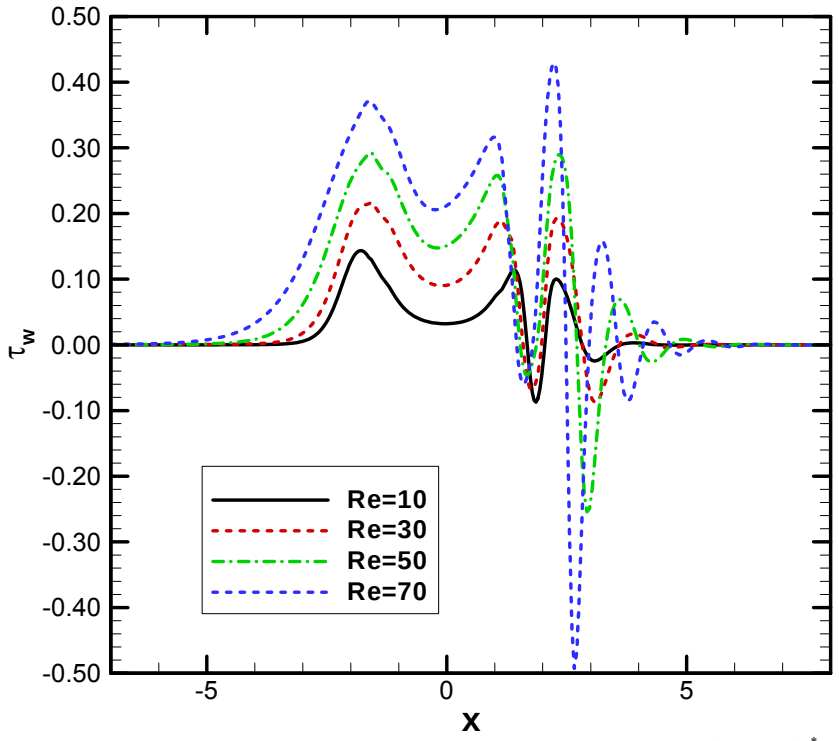

Wall Shear Stress $\tau_w = Ca \frac{\partial u}{\partial x} = \mu \frac{\partial u^*}{\partial x^*} \frac{H}{\sigma_M^*}$

- Wall pressure and shear increase with Re: can affect cells.
- In the front meniscus, both stresses oscillate in the capillary wave.

Unsteady Liquid Plug 2-D Channel: Initial Conditions

Fujioka, Grotberg

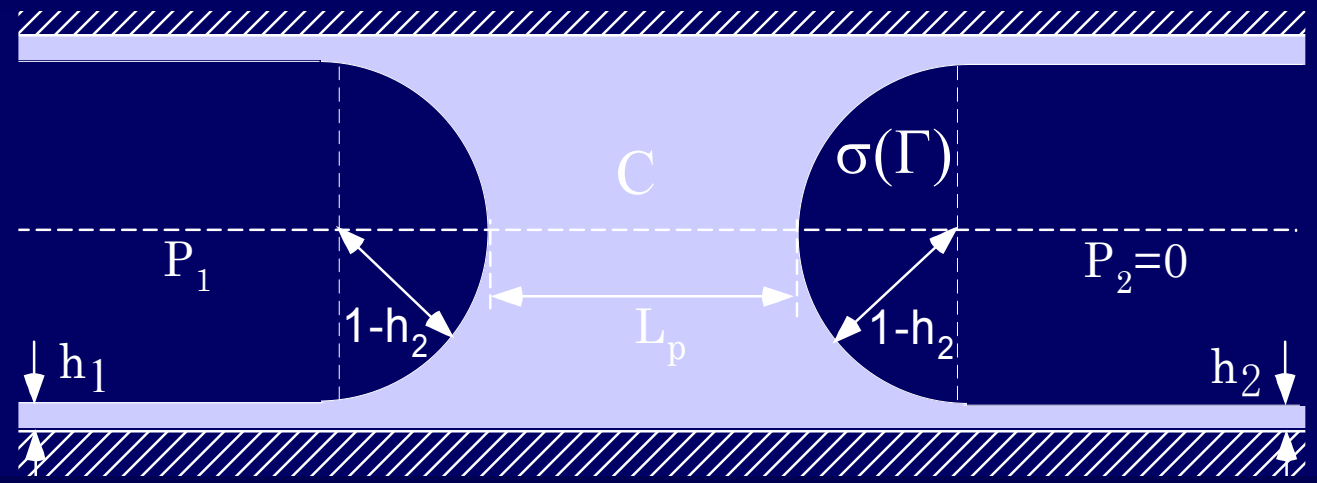

- Hemi-sphere of the radius $1-h_2$, uniform film thickness of $h=h_2$
- Initial velocity and bulk surfactant concentration are $\mathbf{u}=0$ and $C=C_0$ The initial interfacial surfactant concentration in equilibrium with C_0.
- For no surfactant case, $\sigma=1$.

At t=0, a plug of the initial length, $L_P=1$ starts propagating with a constant pressure drop, $\Delta P=P_1-P_2=1$.

Effect of the precursor film thickness on Plug Propagation (no surfactant)

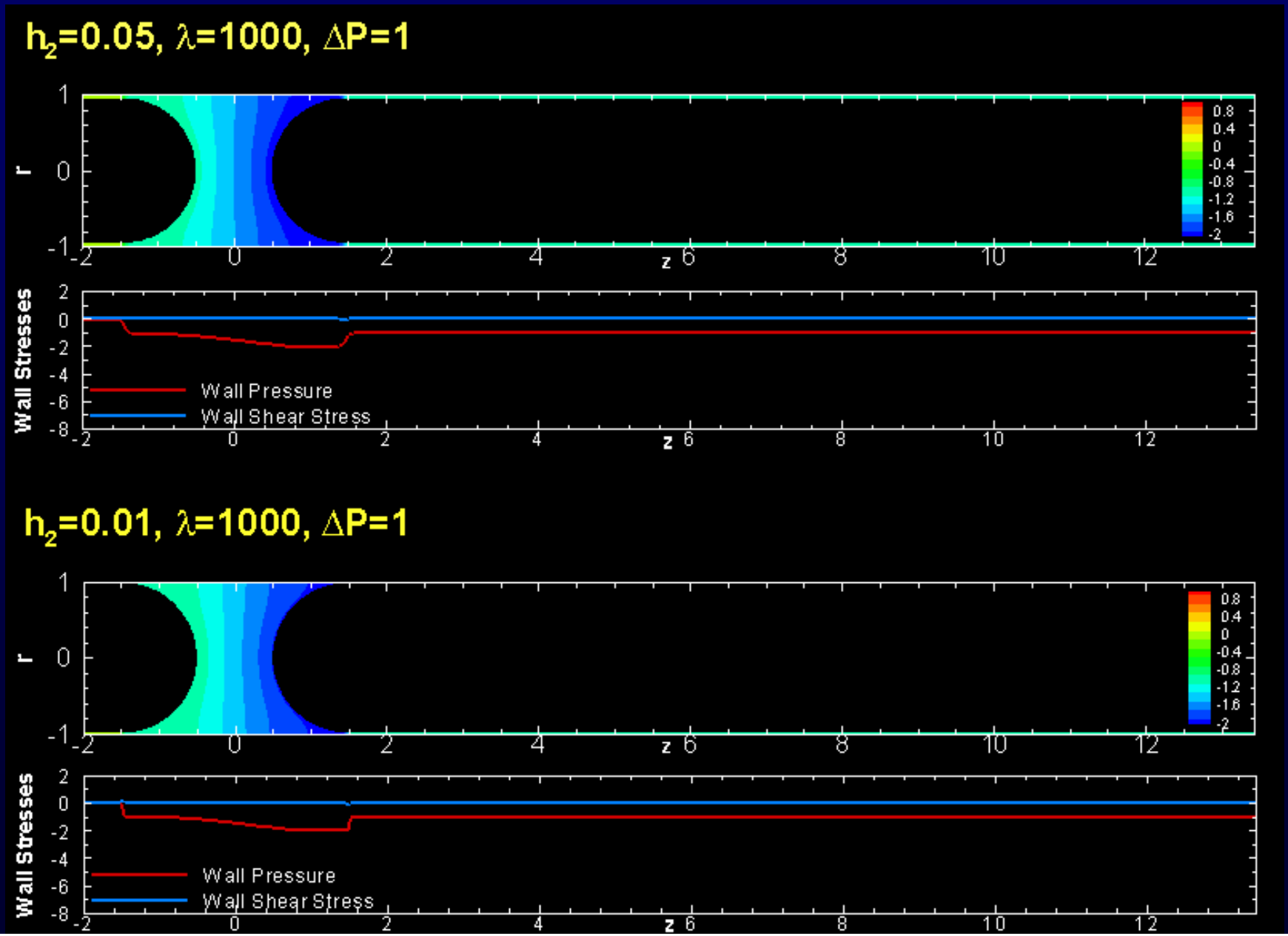

Effect of Surfactant on Plug Propagation

h_2=0.05, λ=1000, ΔP=1 (no surfactant)

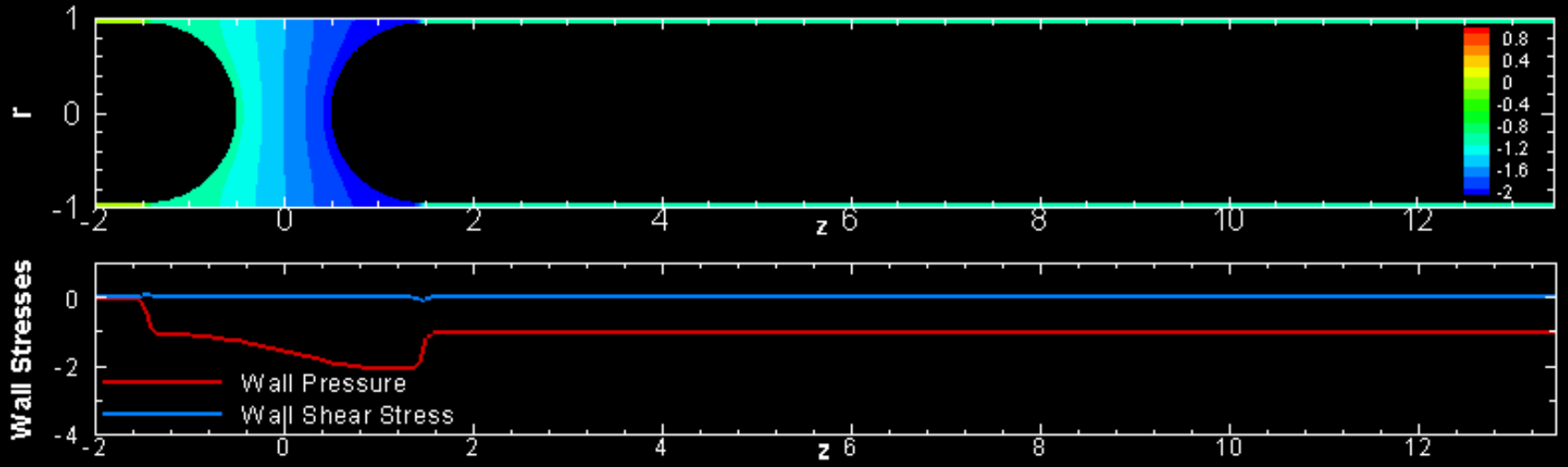

h_2=0.05, λ=1000, ΔP=1, $C_0=10^{-3}$ Sc=10, Sc_s=100, Ka=10^4,Kd=10^2,$\chi=10^{-2}$,E=0.7

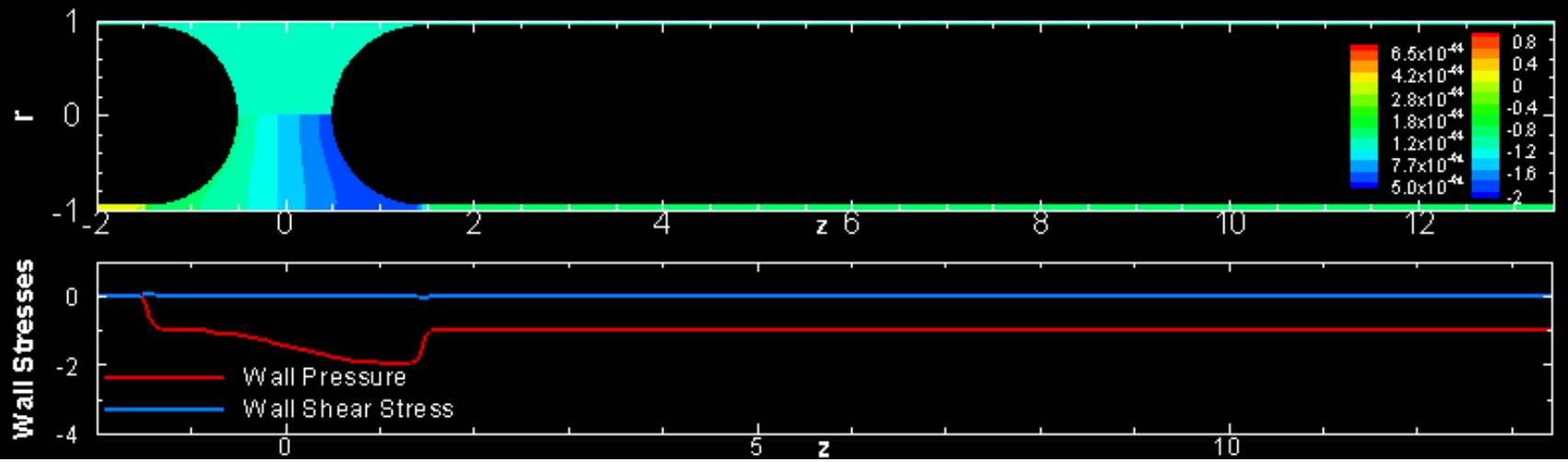

Plug Flow Dynamics Through Bifurcations

Zheng, Fujioka, Grotberg

Plug flows in airways:

- deposits liquid along airway wall.
- splits unevenly at bifurcation.
- determines a final liquid distribution

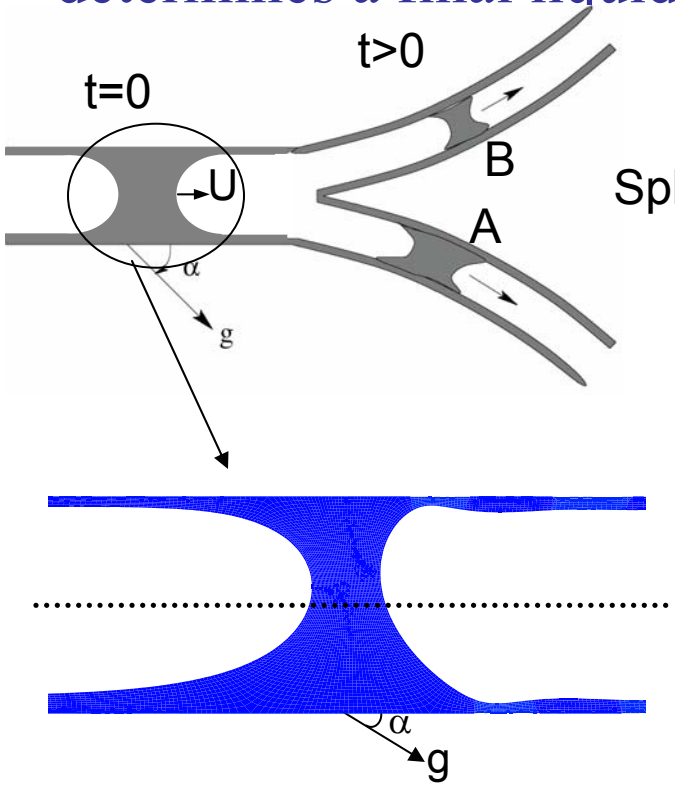

Splitting ratio $R_s = \frac{V_B}{V_A}$

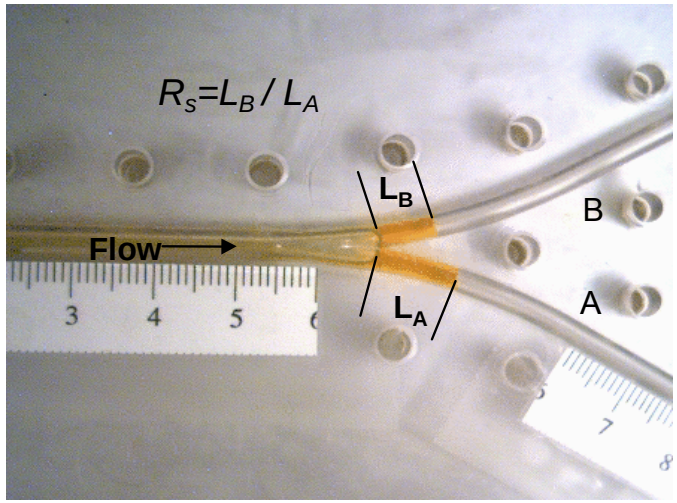

(Y. Zheng, et al. JBE, 2005)

Pre-bifurcation asymmetry

Experimental setup

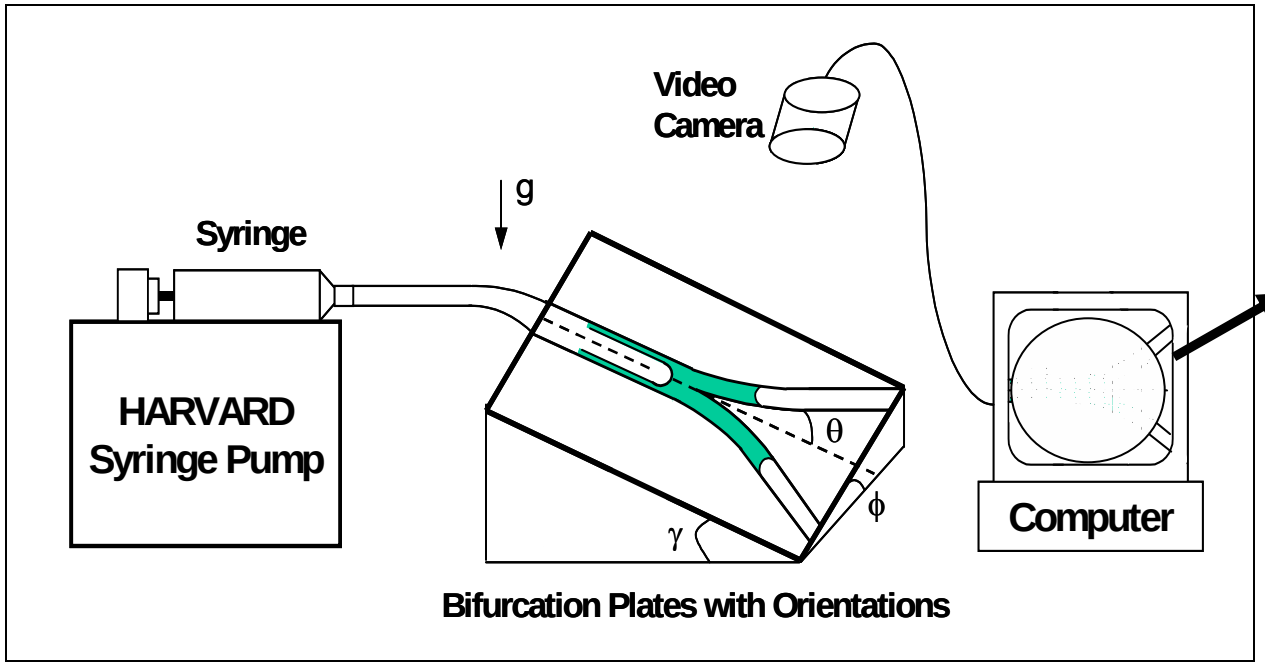

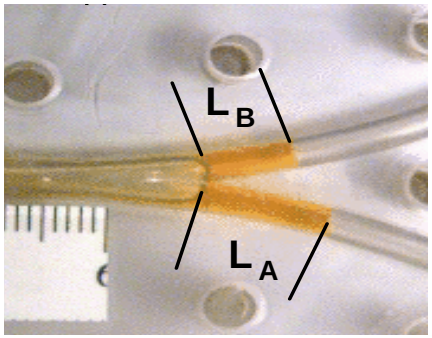

- θ is branching angle of bifurcation, ϕ is roll angle and γ is pitch angle.

  Determine R_s (Ca,Bo, V_p, ϕ, γ) Splitting ratio: $R_s = \frac{L_B}{L_A}$

Simple Theoretical analysis on plug splitting

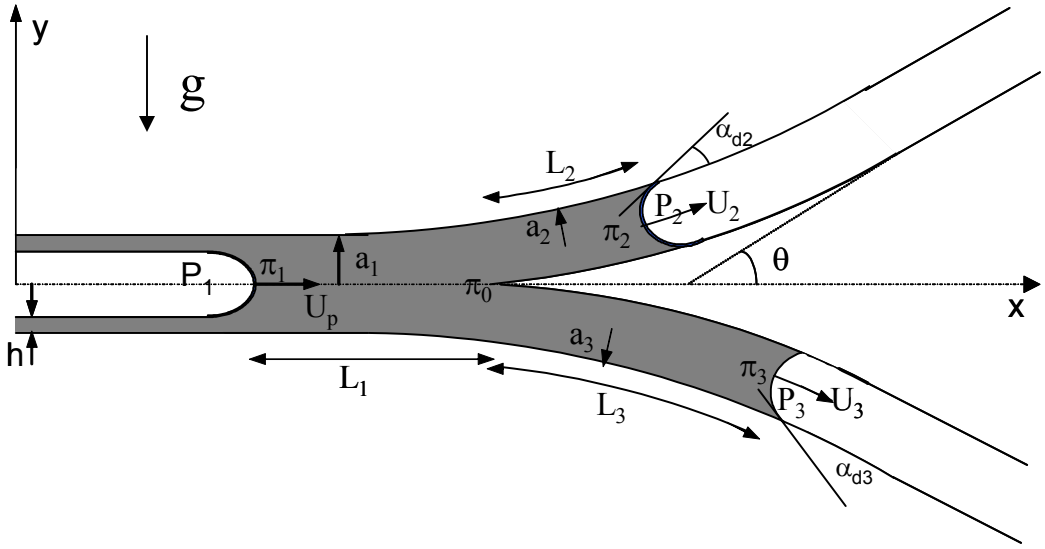

- Compute pressure drops and mass balance between rear and front menisci
- Pressure drops
  - Capillary jump + trailing thin film correction across rear mensicus ($P_1 - \pi_1$)
  - Poiseuille law + gravity in liquid ($\pi_1 - \pi_0$, $\pi_0 - \pi_2$, $\pi_0 - \pi_3$)
  - Moving contact line effect at front menisci. $P_2 - \pi_{2(3)} = (\sigma / a_2)\cos(\alpha_d)$
    - Empirical correlation for α_d $\dfrac{\cos\alpha_s - \cos\alpha_d}{\cos\alpha_s + 1} = 2Ca_L^{1/2}$

(Bracke *et. al.*, *Prog. Coll. Polymer Sci.* 1989)

Results (low Re-low Ca expts.)

Effect of roll angle ϕ and pitch angle γ on Rs vs. Ca

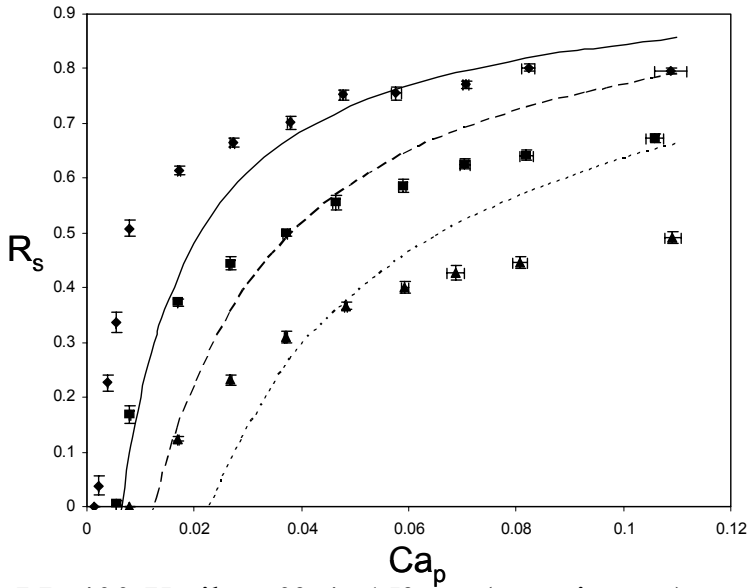

LB-400-X oil, γ=0º. ϕ=15º: ◆ (experiments), —— (theory); ϕ =30º: ■ (experiments), – – – (theory); ϕ =60º: ▲ (experiments), ····· (theory).

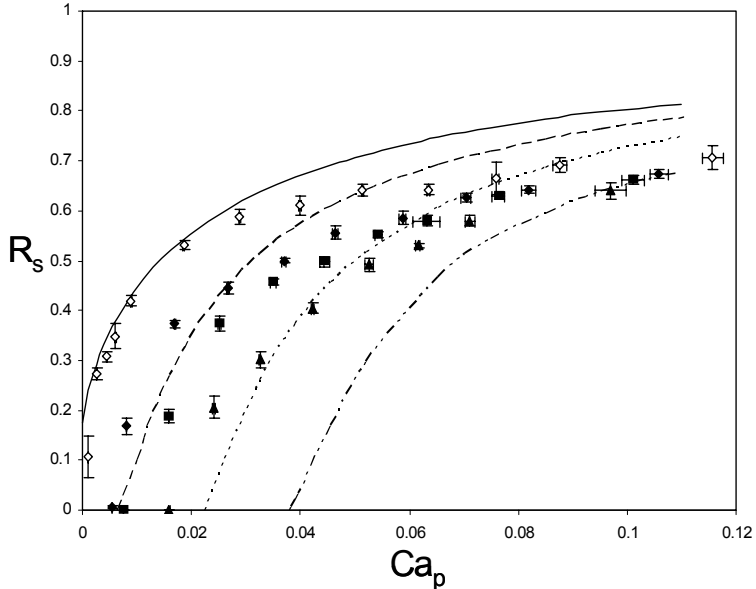

LB-400-X oil, ϕ=30º. γ =-15º: ◇ (experiments), —— (theory); γ=0º: ◆ (experiments), – – – (theory); γ=15º: ■ (experiments), ····· (theory); γ=30º: ▲ (experiments), –·–·– (theory).

- A critical capillary number Ca_c exists below which R_s=0.
- Ca_p increases, R_s increases.
- Larger ϕ and γ cause smaller R_s but larger Ca_c.
- Theory qualitatively agrees with experiments.

Pre-Bifurcation Asymmetry: Gravity Effects

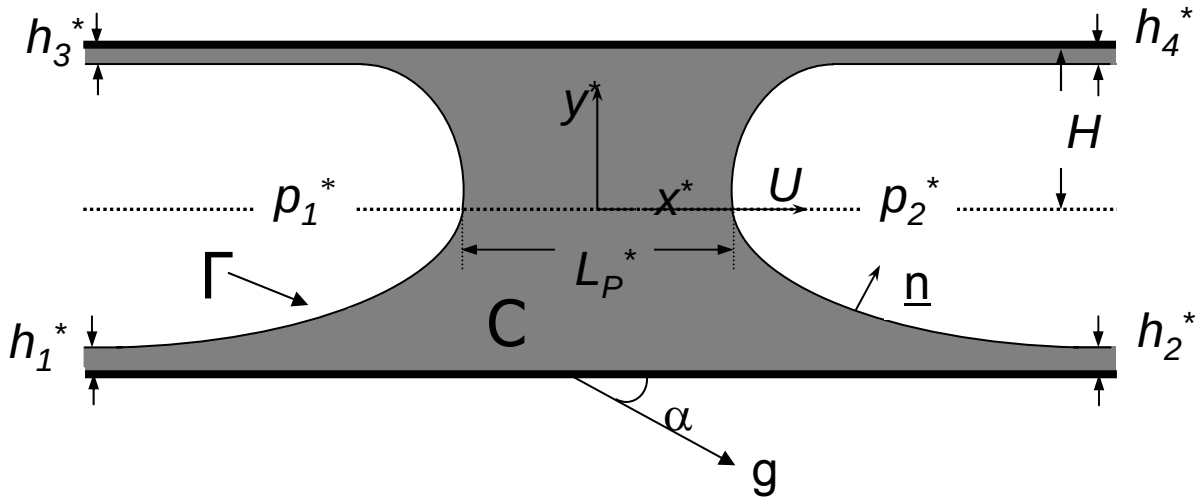

Same governing equations…add gravity → Bo (Bond number)

For steady state require $h_2+h_4=h_1+h_3$

Bo=0, No Gravity

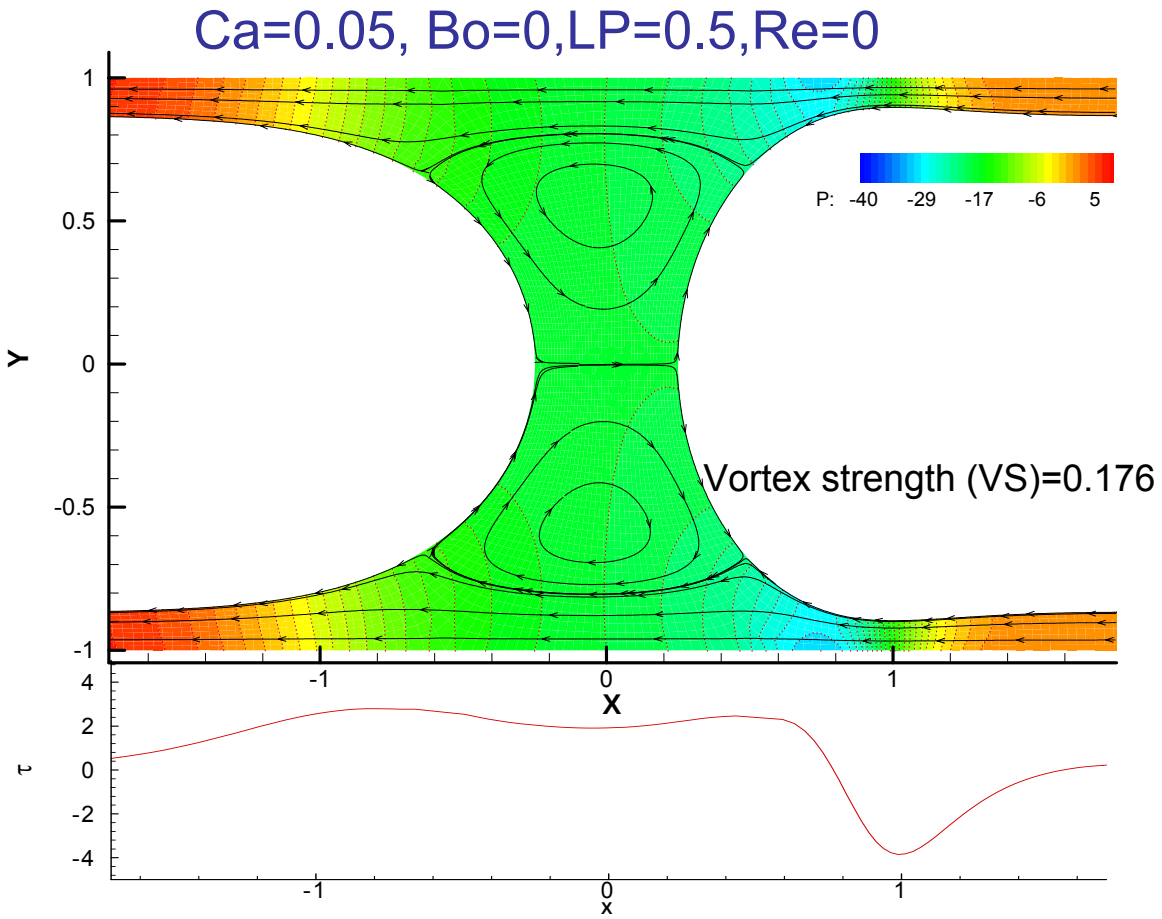

- Two symmetric recirculation regions.
- Precursor film fluid flows into trailing film

Bo=0.1, 0.6

α=90°

Ca=0.05, Bo=0.1,LP=0.5,Re=0

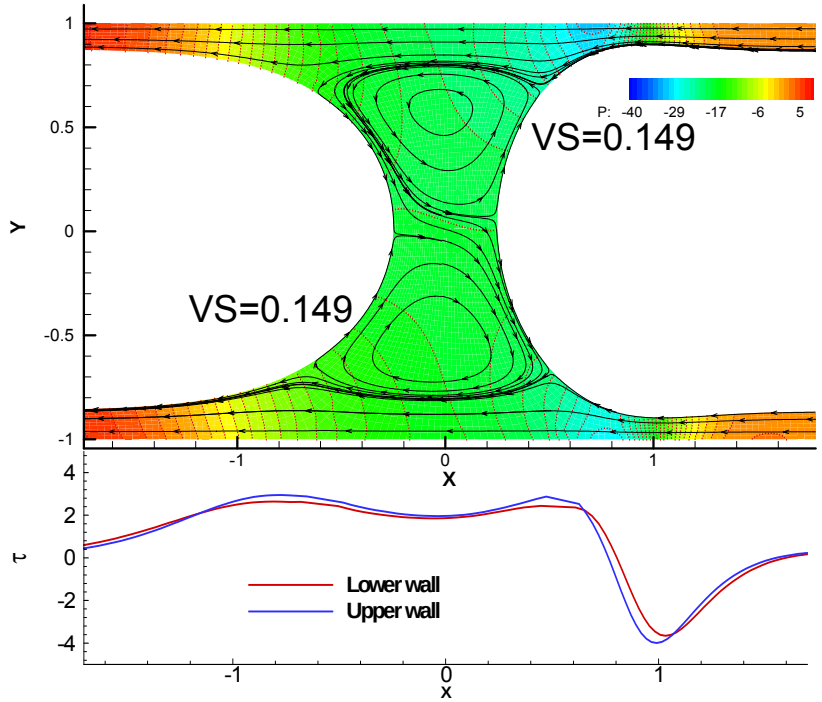

Ca=0.05, Bo=0.6,LP=0.5,Re=0

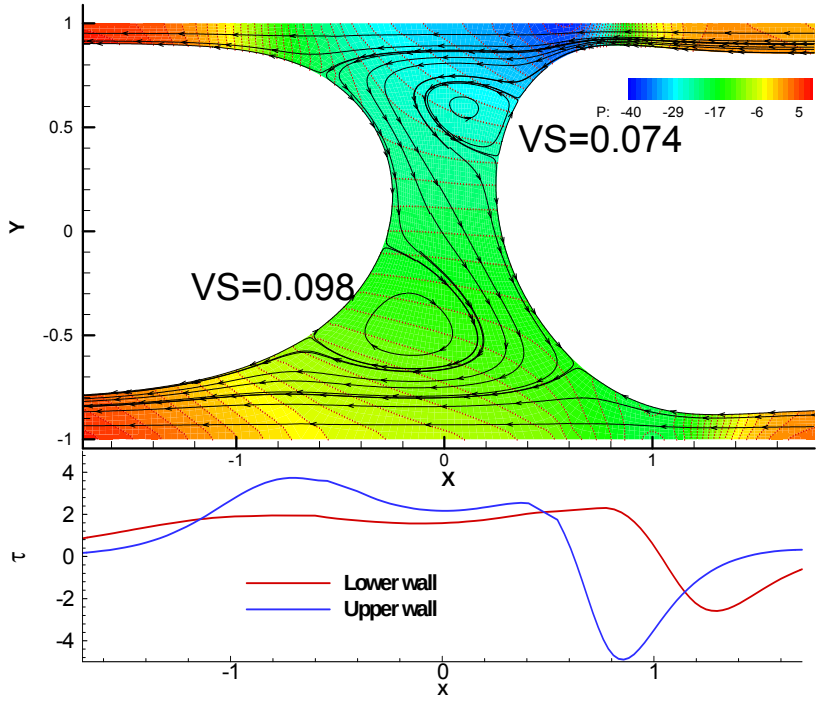

- Bypass flow from upper precursor film to lower trailing film.
- Recirculation decreases with increasing Bo.
- Lower (upper) wall shear stress decreases (increases).

Effects of Ca for Re=0

Ca=0.03, Bo=0.6,LP=1,Re=0 $\alpha=90°$ Ca=0.3, Bo=0.6,LP=1,Re=0

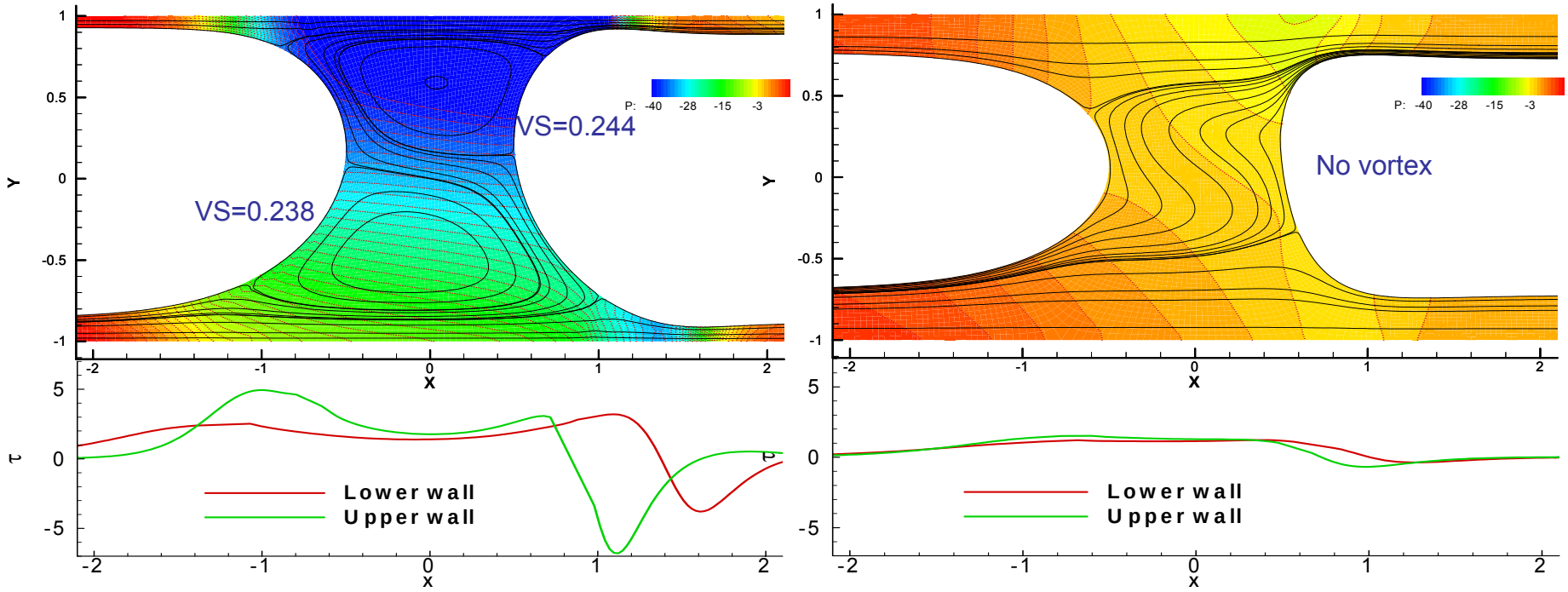

- Recirculation decreases with increasing Ca.
- No recirculations for high Ca, high Bo.
- Wall shear decreases with increasing Ca.

Effect of Re

Ca=0.05, Bo=0.6,LP=0.5,Re=50 $\alpha=90°$ Ca=0.05, Bo=0.6,LP=2.0, Re=50

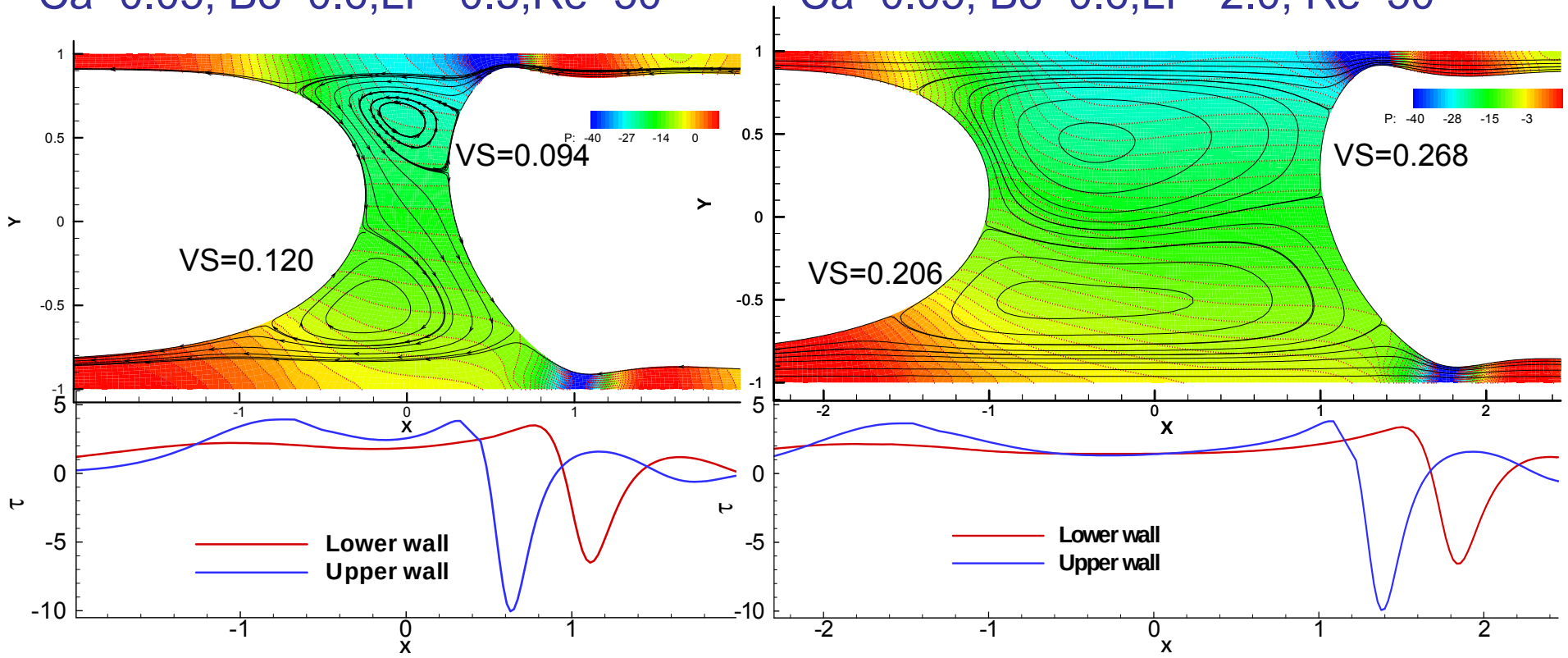

- Recirculations increase and shift to left with increasing Re.
- The streamline pattern is similar.
- Shear stress increases with Re.

Effects of surfactant

Ca=0.05, Bo=0.6,LP=0.5,Re=0, E=0.7, C0 = 10^{-4} α=90°

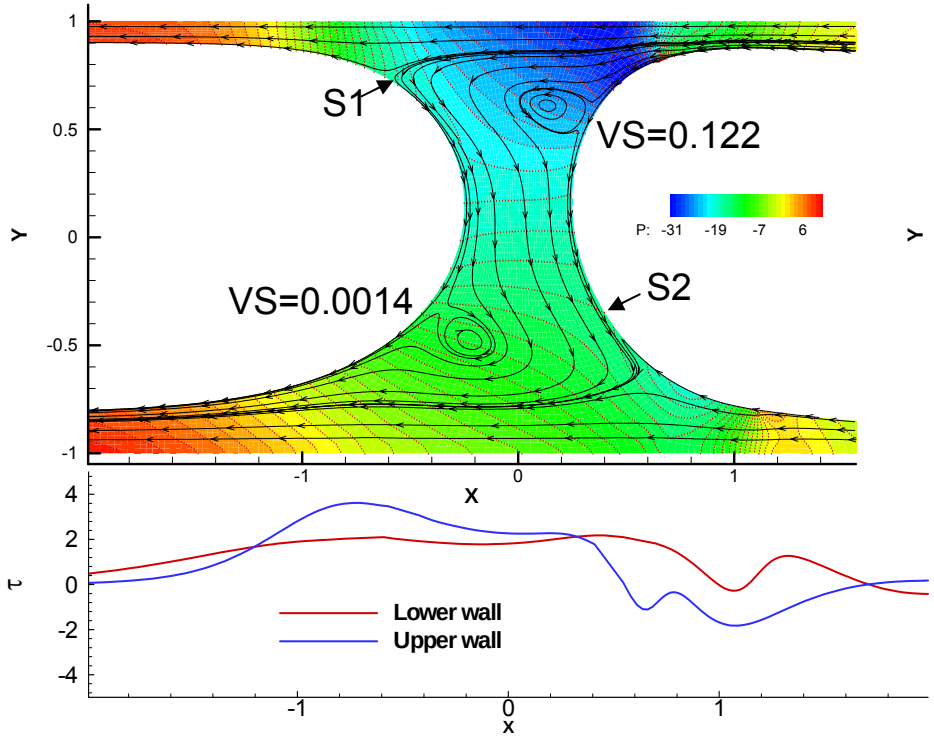

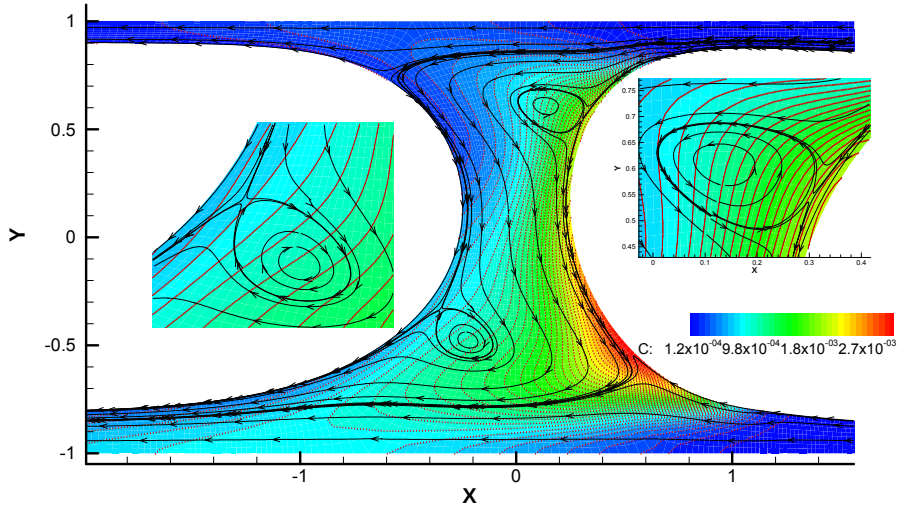

Color: surfactant concentration contour

- Recirculations are weaker with soluble surfactant (E=0.7).
- Saddle points exist inside the plug core.
- Surfactant accumulates at the lower front transition region.

Cellular Damage Induced by Liquid Plug Propagation and Rupture in a Microfluidic Airway System

Dongeun Huh, Hideki Fujioka, James B. Grotberg & Shuichi Takayama

Department of Biomedical Engineering

Department of Macromolecular Science and Engineering

University of Michigan, Ann Arbor

Micro-engineered *In Vitro* Small Airway System

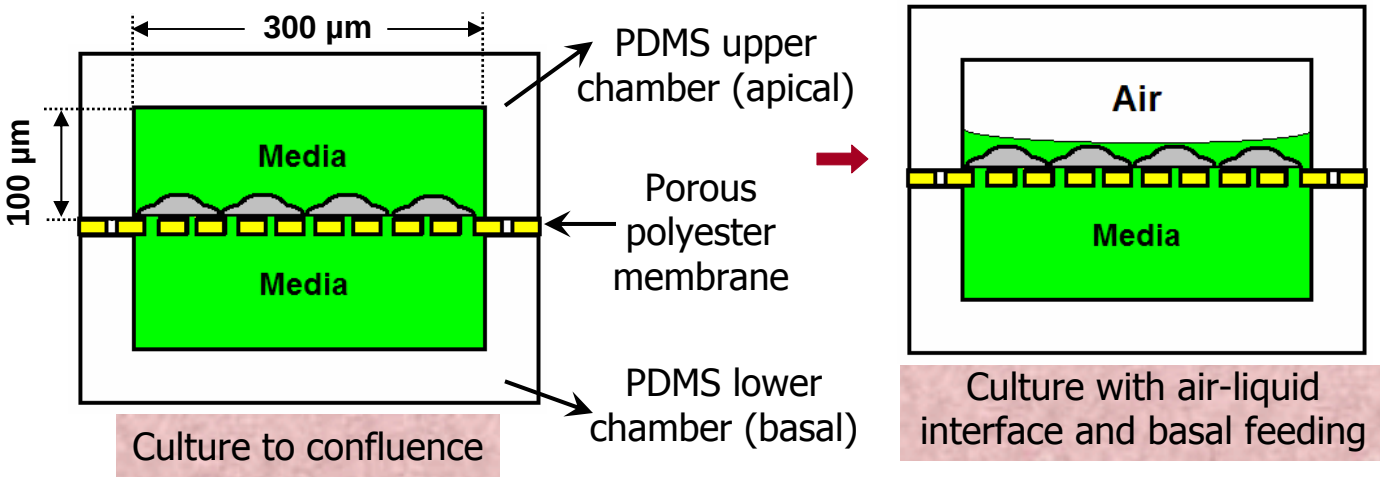

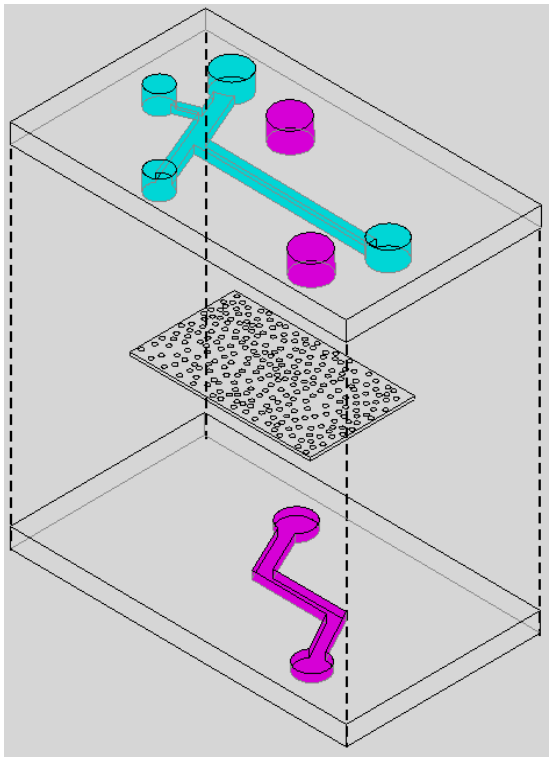

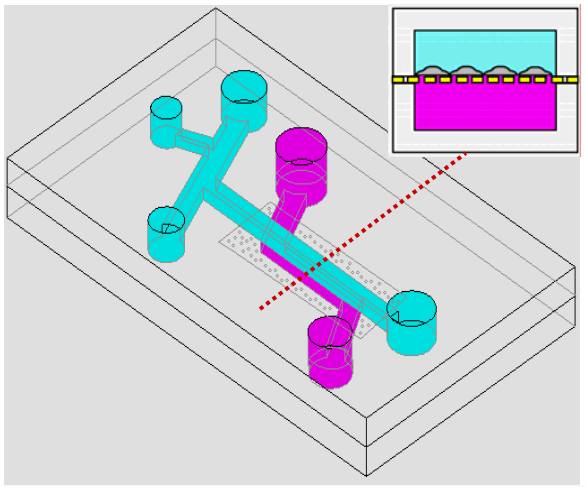

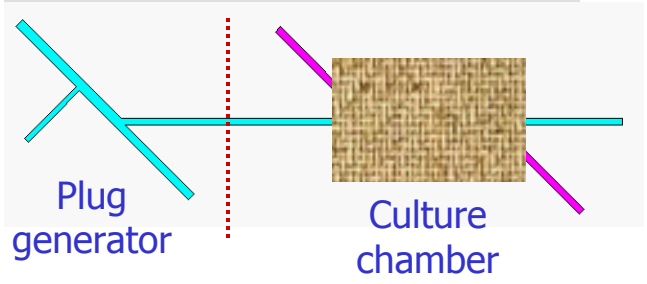

Liquid perfusion culture

Air-liquid interface (ALI) culture

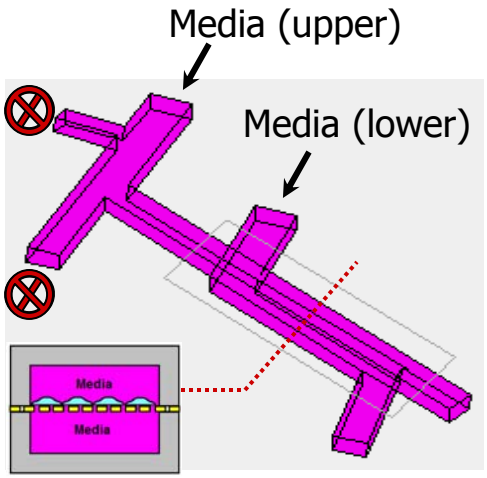

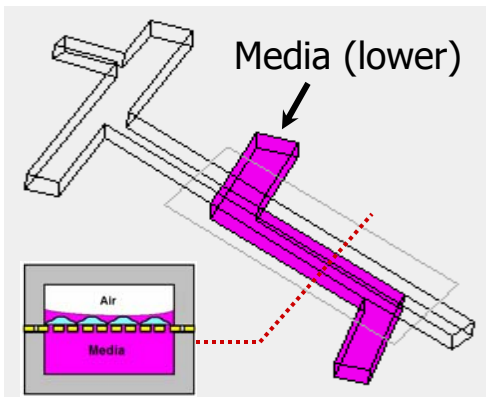

Micro-engineered *In Vitro* Small Airway System

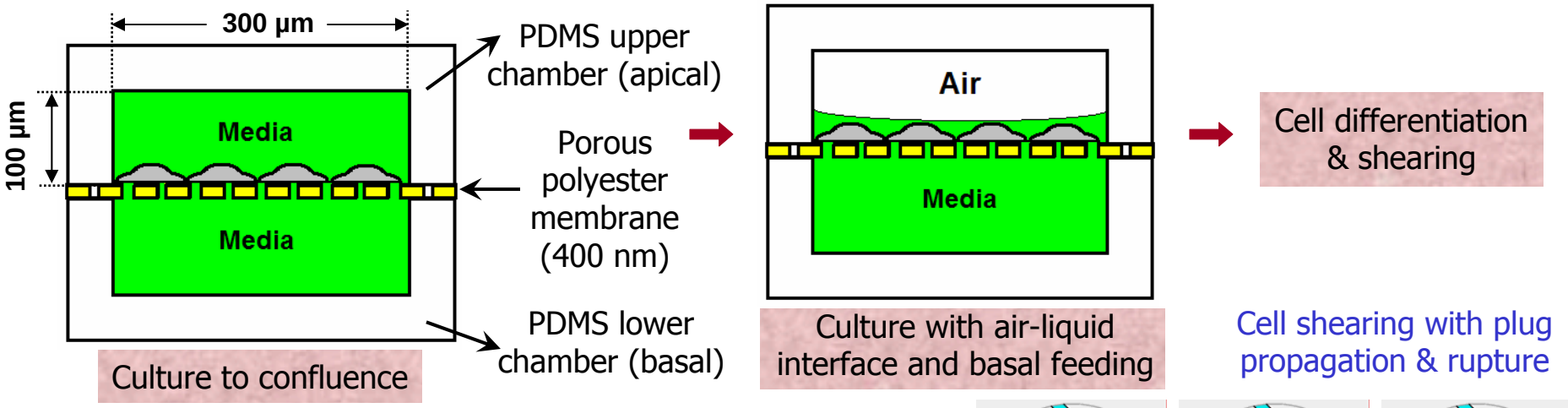

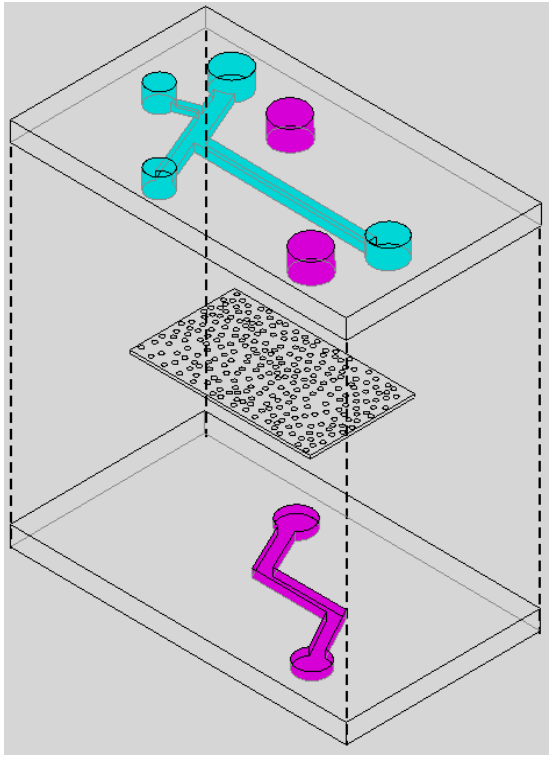

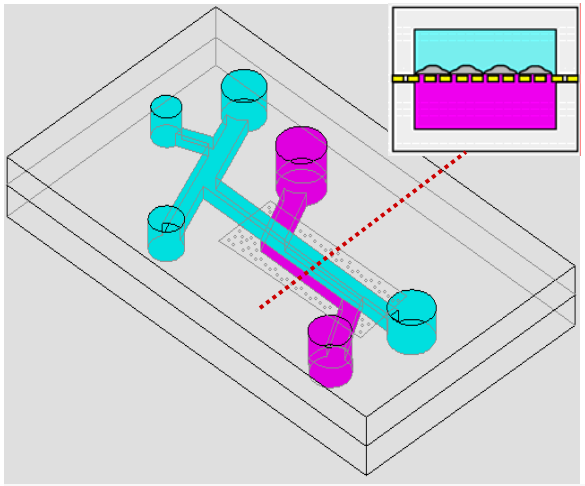

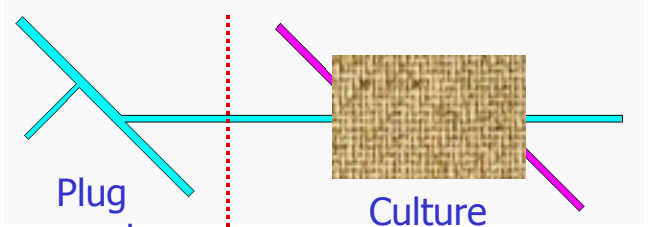

Cell shearing with plug propagation & rupture

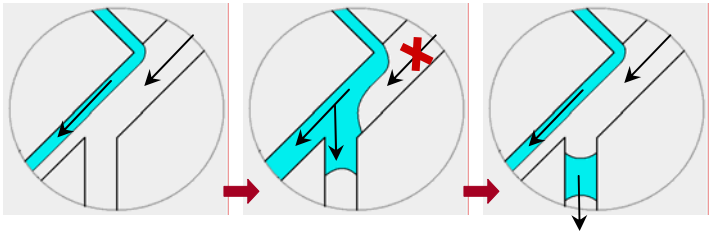

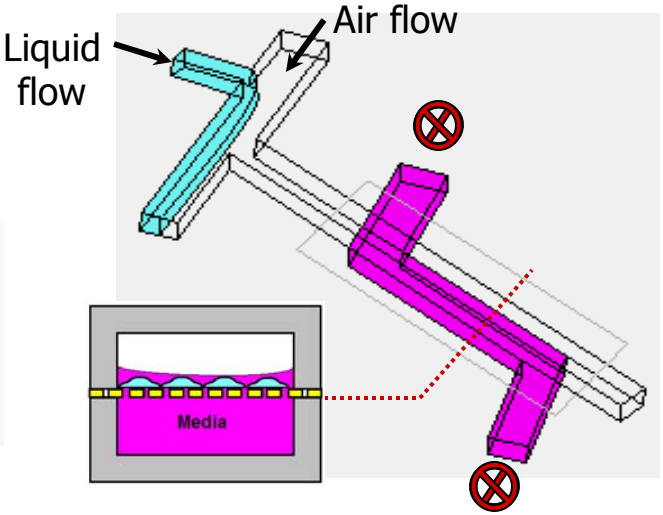

Detrimental Effect of Plug Rupture

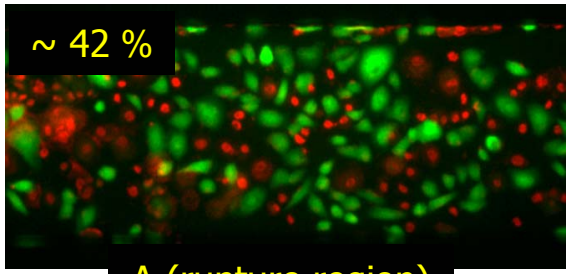

A (rupture region)

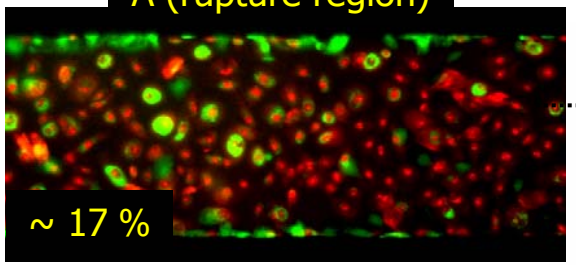

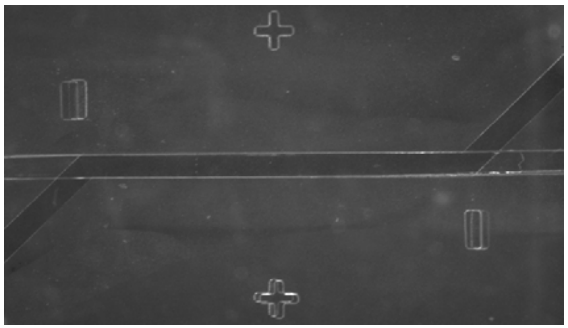

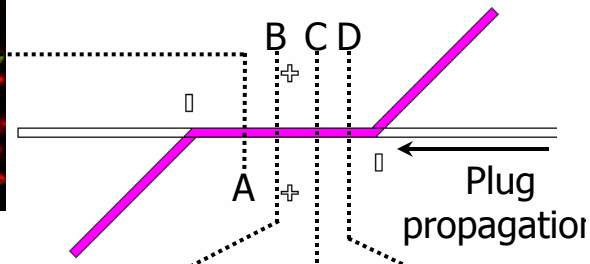

Viability from A ⟺ Average viability from B, C, D

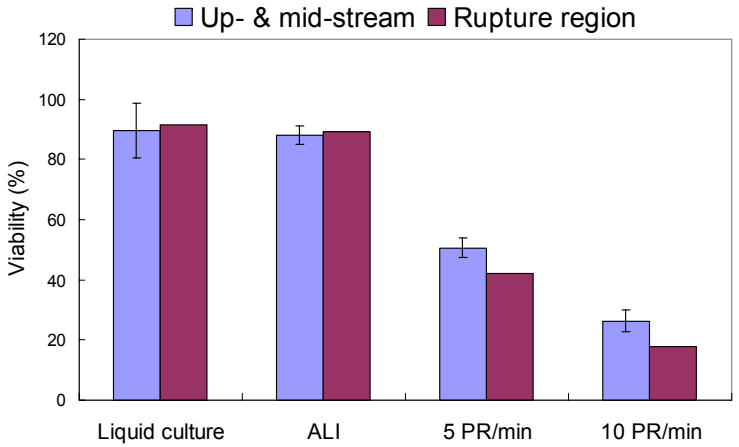

8 % (5 PR/min) or 9 % (10 PR/min) lower in rupture region

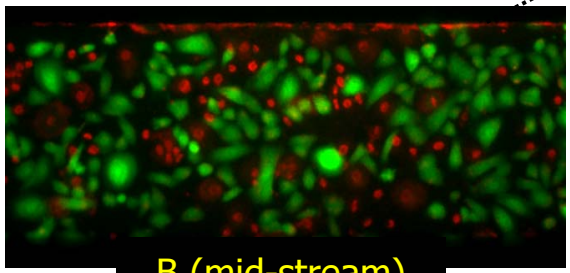

B (mid-stream)

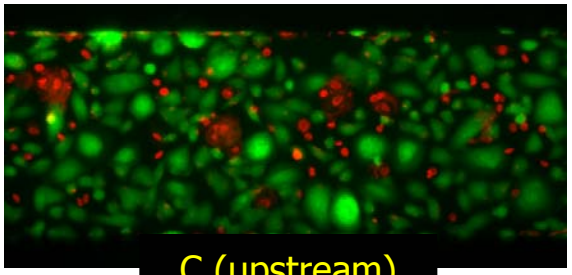

C (upstream)

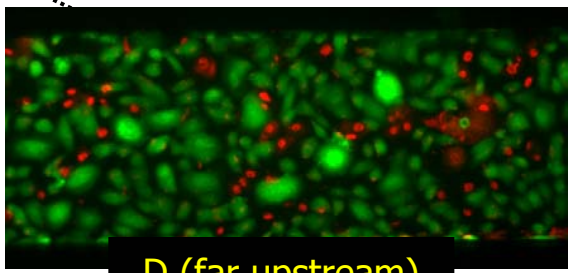

D (far upstream)

5 PR/min

~ 50 %

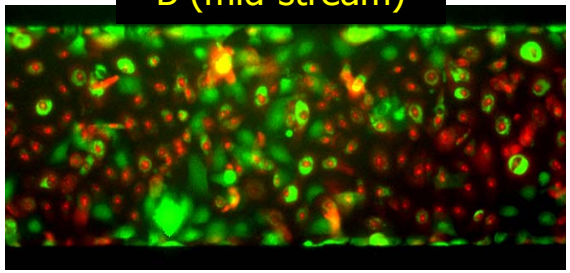

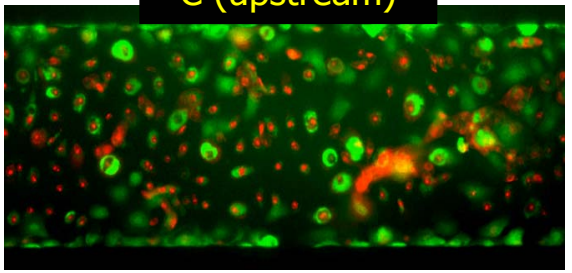

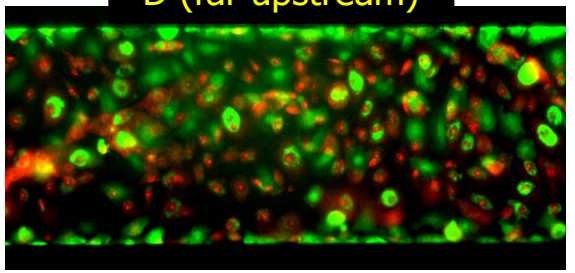

10 PR/min

~ 26 %

Surfactant Spreading on a Thin Viscous Film

- Drops of surface active substances land on the lungs air-liquid interface:
  - Oil Fog, Surfactant Aerosol, Drugs
- Fronts of surface active substances are introduced into airways (last step to alveoli)
  - Surfactant Instillation, Other Ingestions
- How do they spread?
- Answering this question led to identifying a new fluid-dynamical shock wave

Steady Surfactant "Spreading" Model

Borgas & Grotberg, JFM 1988

Steady state "spreading" model

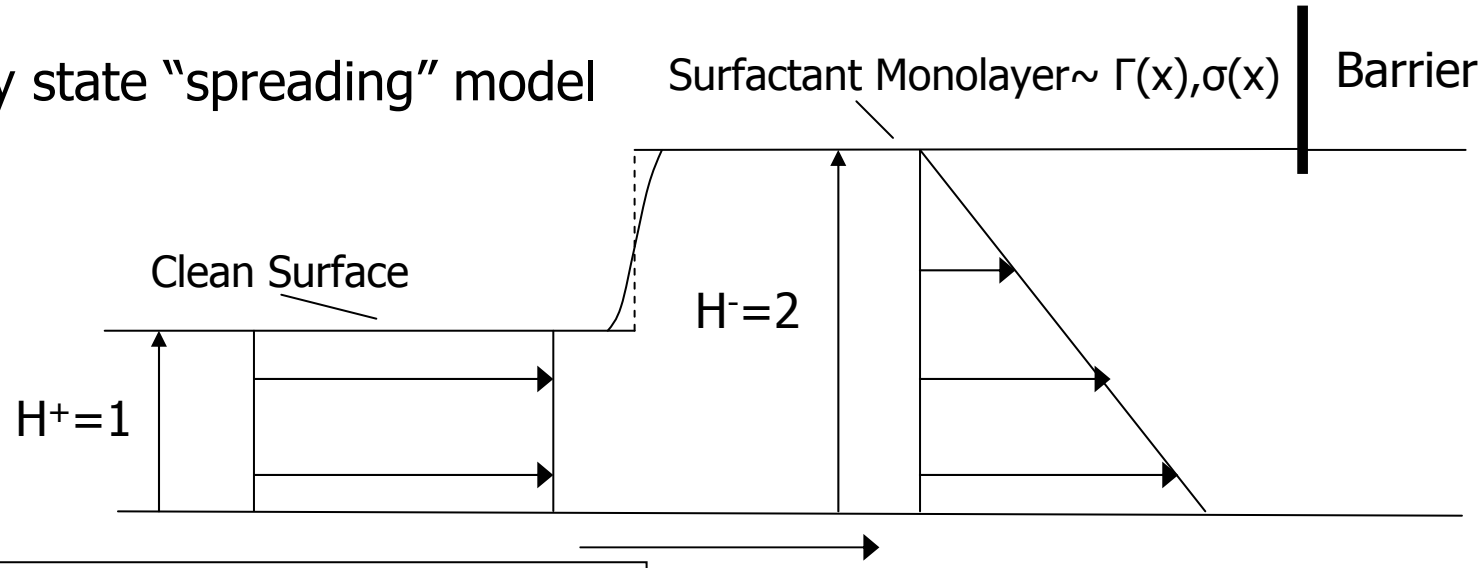

$$-\tfrac{1}{3}\,p_x H^3 + \tfrac{1}{2}\,\sigma_x H^2 + H = 1$$

$$(-\tfrac{1}{2}\,p_x H^2 + \sigma_x H + 1)\Gamma = \frac{1}{Pe_s}\,\Gamma_x$$

$$p_x = -\varepsilon^2(\sigma H_{xx})_x, \quad \varepsilon = \frac{H}{L}$$

Lubrication theory ($\varepsilon \to 0$), $p_x \sim 0$, no diffusion ($Pe_s \to \infty$)

$$\sigma_x = -\tfrac{1}{2}, \quad u_s(x) = 0, \quad H(x) = 2$$

Shock

Unsteady, Axisymmetric Surfactant Monolayer Spreading on a Thin Film

Evolution Equations

$$\frac{\partial H}{\partial t} = \frac{1}{r}\frac{\partial}{\partial r}\left\{r\left[\frac{1}{3}\frac{\partial P}{\partial r}H^3 - \tfrac{1}{2}H^2\frac{\partial \sigma}{\partial \Gamma}\frac{\partial \Gamma}{\partial r}\right]\right\},$$

$$\frac{\partial \Gamma}{\partial t} = \frac{1}{r}\frac{\partial}{\partial r}\left\{r\left[\left(\frac{1}{Pe} - \Gamma H\frac{\partial \sigma}{\partial \Gamma}\right)\frac{\partial \Gamma}{\partial r} + \frac{\partial P}{\partial r}\tfrac{1}{2}\Gamma H^2\right]\right\}.$$

$$P(r,z,t) = G[H(r,t)-z] - \epsilon^2\beta\left[\frac{\partial^2 H}{\partial r^2} + \frac{1}{r}\frac{\partial H}{\partial r}\right]$$

Same assumptions as before, shock wave develops

Shock speed given in terms of jump in volume flow rate divided by jump in cross-sectional area of the film

$$\frac{dr_f}{dt} = \frac{2\pi r_f\left(\frac{1}{2}v_s^- H^- - \frac{1}{2}v_s^+ H^+\right)}{2\pi r_f\left(H^- - H^+\right)} = \frac{\frac{1}{2}v_s^- H^-}{\left(H^- - H^+\right)}$$

but, $\dfrac{dr_f}{dt} = v_s^- \quad \rightarrow \quad H^- = 2 \quad$ when $\quad H^+ = 1$

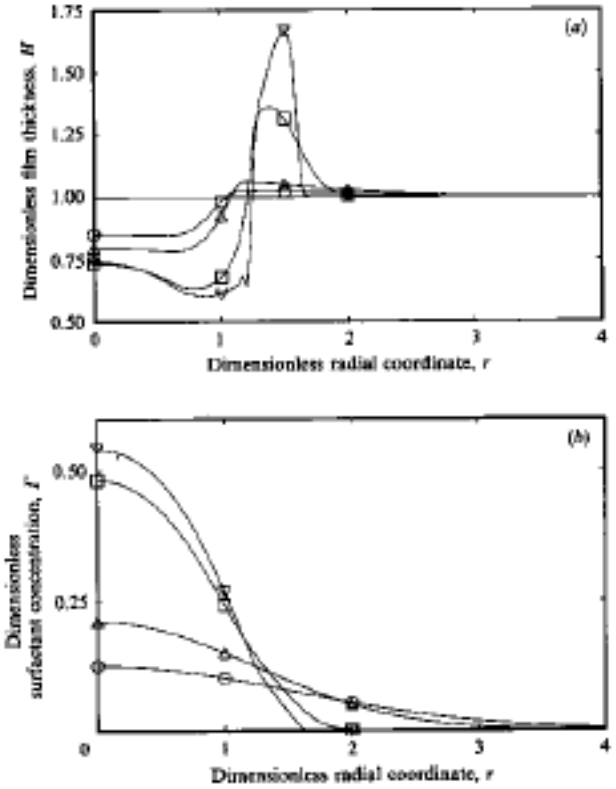

FIGURE 4. Film thickness and surfactant concentration profiles for ○, $Pe = 0.5$; △, $Pe = 1.0$; □, $Pe = 10.0$; ▽, $Pe = 100.0$. $G = 0$, $\beta = 5.0$, $RI = 0.7$, $\Gamma_{max} = 1.0$ and $t = 0.5$.

Gaver & Grotberg, JFM 1990

Surface Speed and Critical Thinning Behind Shock

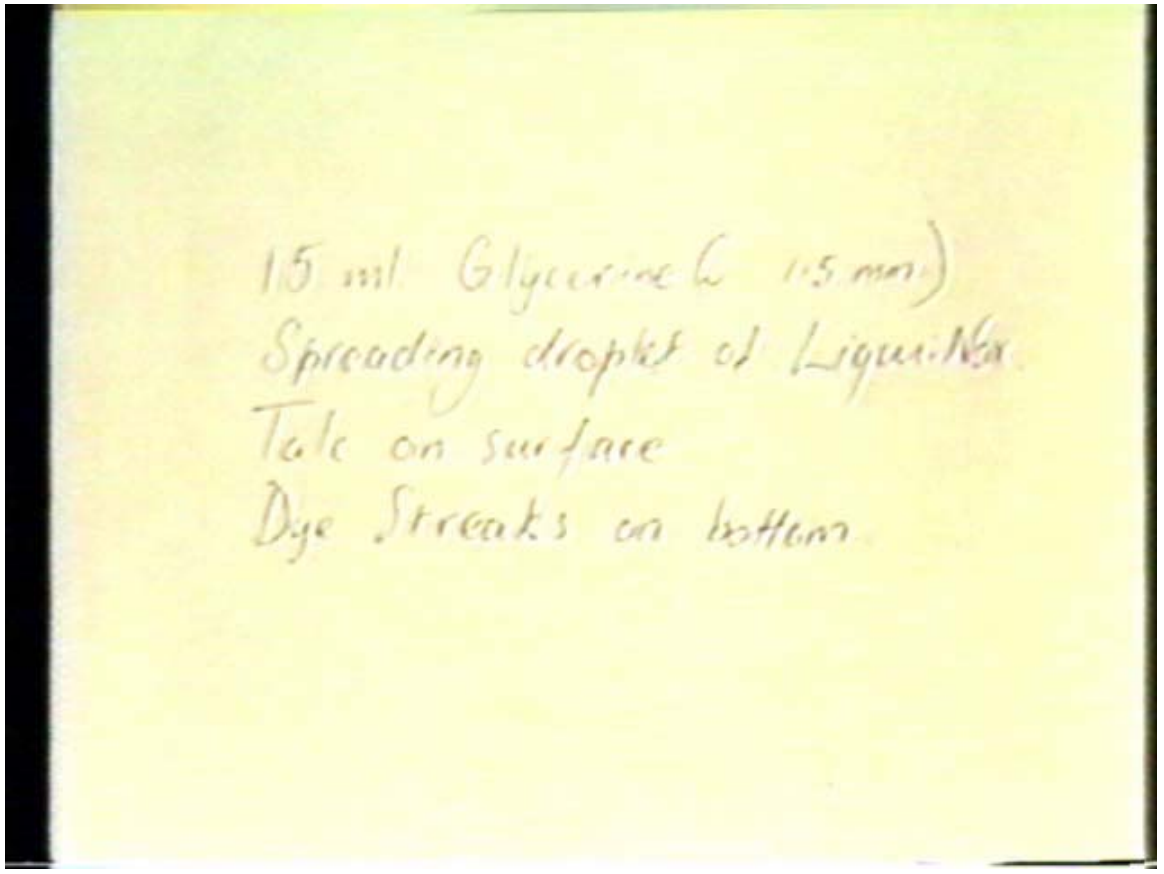

Gaver & Grotberg, JFM 1992

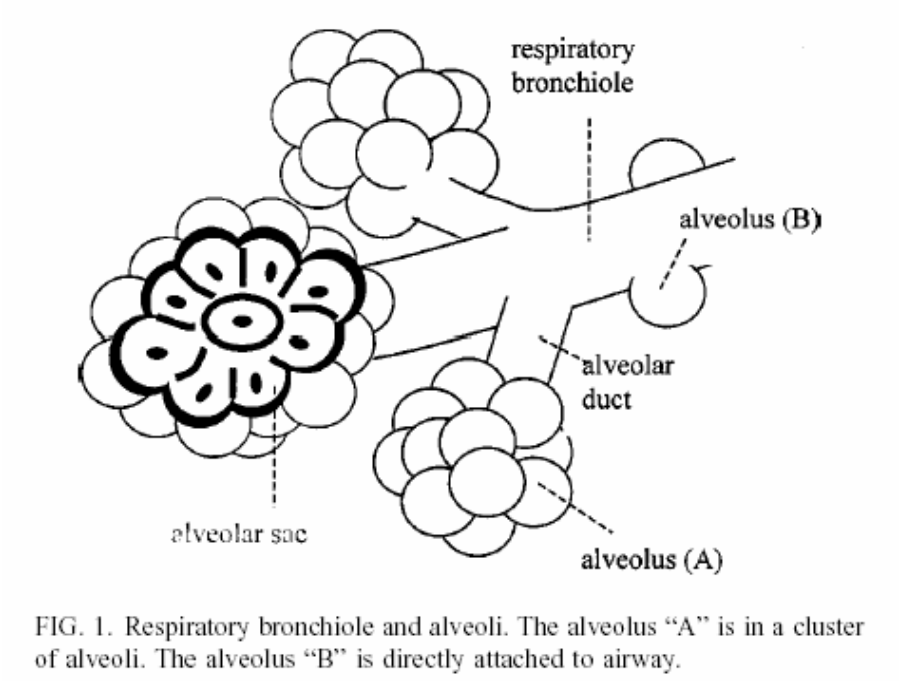

FIG. 1. Respiratory bronchiole and alveoli. The alveolus "A" is in a cluster of alveoli. The alveolus "B" is directly attached to airway.

Cycle-Induced Flow and Surfactant Transport in an Alveolus

Wei, Fujioka, Grotberg PoF 2005

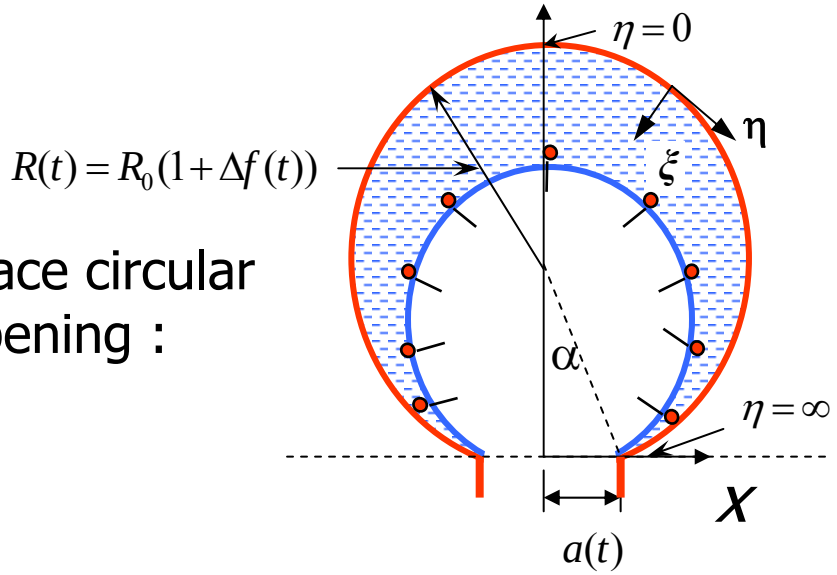

- "High surface tension" ~ interface circular
- The bc's of Γ at the alveolar opening :

(i) No flux $\partial\Gamma/\partial s = 0$

(ii) Fixed Γ=1

Velocity Field: Stokes Flow

Stream Function Formulation

$$\nabla^2\nabla^2\psi = 0 \qquad \nabla^2 = \frac{(\cosh\eta - \cos\xi)^2}{a(t)^2}\left(\frac{\partial^2}{\partial\xi^2} + \frac{\partial^2}{\partial\eta^2}\right)$$

bipolar coordinates

Assume (following Haber et al)

$$\psi = \psi_1 + \psi_2$$

ψ_1 represents the flow contribution without the alveolar wall while ψ_2 is the disturbance flow field caused by the alveolar boundary.

After imposing BCs

$$\psi_1 = Q\left[1 - \frac{2}{\pi}\left(\sin^{-1} Z - Z(1-Z^2)^{1/2}\right)\right] - a\dot{a}xy,$$

$$Z = \frac{1}{a(t)\sqrt{2}}\left[a^2 - x^2 - y^2 + \sqrt{(x^2+y^2-a^2)^2 + 4y^2}\right]^{1/2}.$$

first and the second terms are the 2-D Sampson flow [11, 12] and a

$$\psi_2 = \frac{1}{(\cosh\eta - \cos\xi)}\sum_{n=1}^{\infty}\hat{\phi}_n(\xi)\sin(k_n\eta),$$

$$\hat{\phi}_n = A_n\left[\frac{\cos(\xi-\xi_2)\sinh(k_n(\xi-\xi_2))}{\cos(\xi_1-\xi_2)\sinh(k_n(\xi_1-\xi_2))} - \frac{\sin(\xi-\xi_2)\cosh(k_n(\xi-\xi_2))}{\sin(\xi_1-\xi_2)\cosh(k_n(\xi_1-\xi_2))}\right] +$$
$$B_n\left[\frac{\cos(\xi_1-\xi)\sinh(k_n(\xi_1-\xi))}{\cos(\xi_1-\xi_2)\sinh(k_n(\xi_1-\xi_2))} - \frac{\sin(\xi_1-\xi)\cosh(k_n(\xi_1-\xi))}{\sin(\xi_1-\xi_2)\cosh(k_n(\xi_1-\xi_2))}\right] +$$
$$C_n\left[\cos(\xi\text{-}\xi_1)\frac{\sinh(k_n(\xi-\xi_2))}{\sinh(k_n(\xi_1-\xi_2))}\right] + D_n\left[\cos(\xi_2\text{-}\xi)\frac{\sinh(k_n(\xi_1-\xi))}{\sinh(k_n(\xi_1-\xi_2))}\right],$$

The effect of soluble surfactant

- Conservation of bulk surfactant
- Conservation of interfacial surfactant
- SBCs normal (capillarity), tangential (Marangoni)
- Bulk diffusion "fast", C=1
- Sorption controlled

$$K = \frac{a_0 k_d}{U}$$

Sorption Parameter

Competing Effects:

- Wall motion
- Pressure/capillarity
- Marangoni (interfacial gradients of Γ and σ)

Instantaneous Streamlines

Inhalation

Exhalation

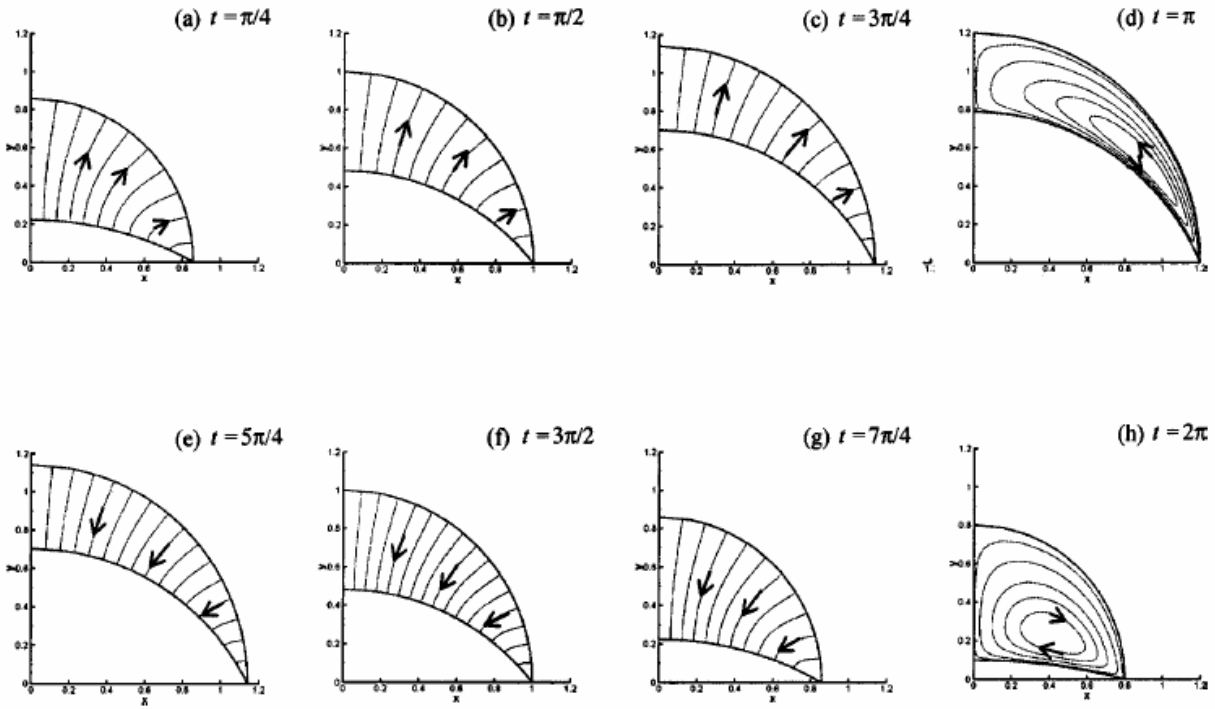

FIG. 3. Snapshots of streamlines during a breathing cycle for the type A alveolus in the presence of an insoluble surfactant. $V=0.9$, $\Delta=0.2$, $\alpha=\pi/2$, Ma $=4$, $\mathrm{Pe}_s=10$, and $I:E=1:1$. The alveolus expands during inspiration [(a)–(d)], while it contracts during expiration [(e)–(h)]. (d) corresponds to the moment of the end of inspiration and (h) is at the end of expiration. Though the alveolus has no motions at the instant of (d) and (h), there are still flows induced by the Marangoni stresses via nonuniform surfactant concentrations along the interface.

Flow is mostly "reversible" during inhalation vs. exhalation

Not "reversible" at turn-around

- Opposite recirculation directions
- Thinner vs thicker layer

Cycle-Averaged Streamlines – K=0 (Insoluble Surfactant)

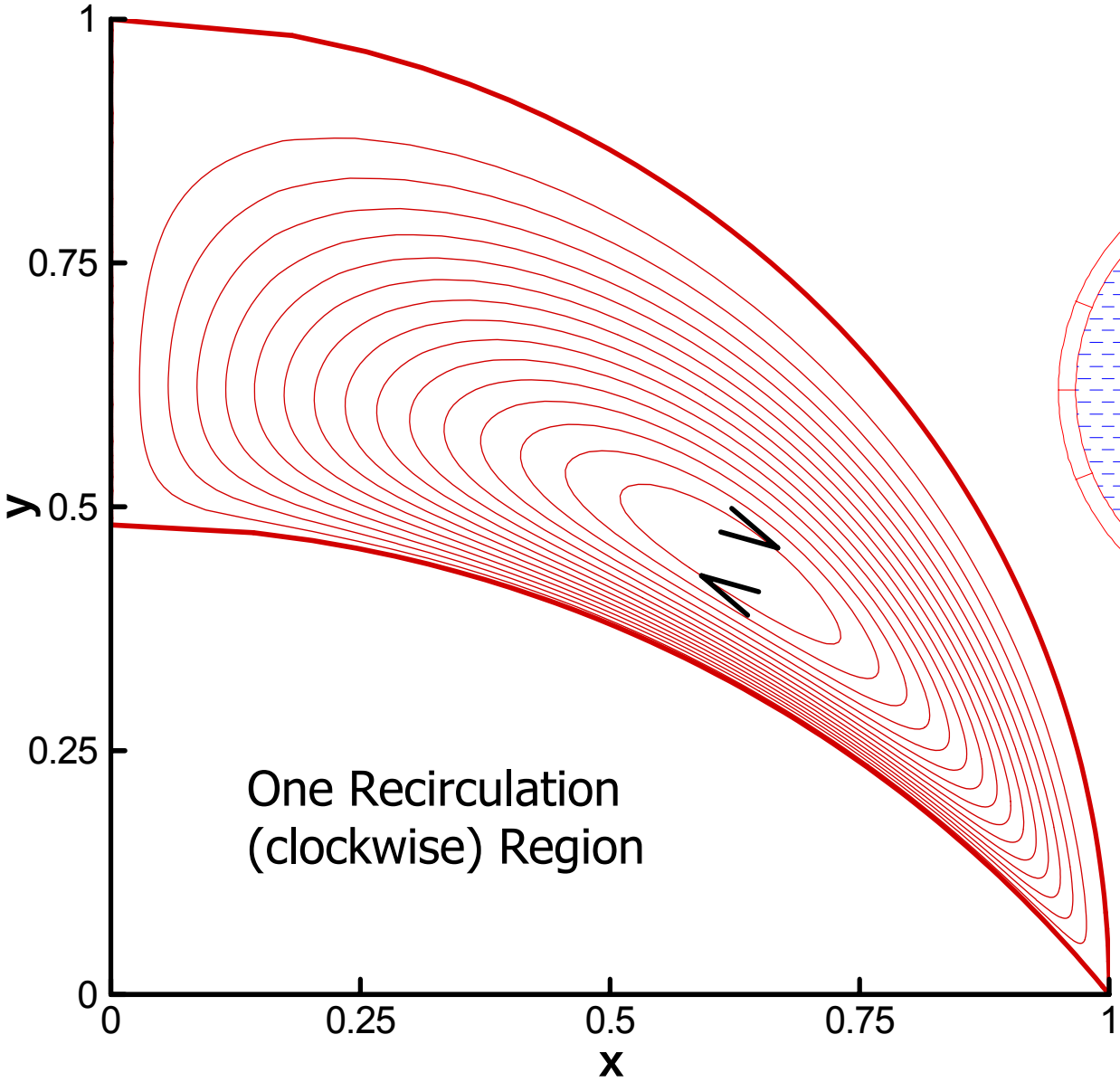

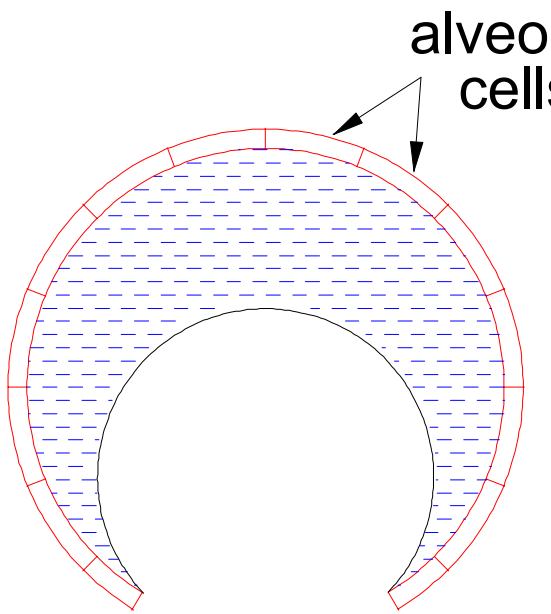

Mixing & Cell-Cell Communication

- **fixed end conc.**
- **I:E =1:1)**

V=0.9, Δ=0.2, $\alpha=\pi/2$, Ma=4.0, Ps=10.0, K=0 (insoluble)

Cycle-Averaged Streamlines - K=0.5 (Soluble)

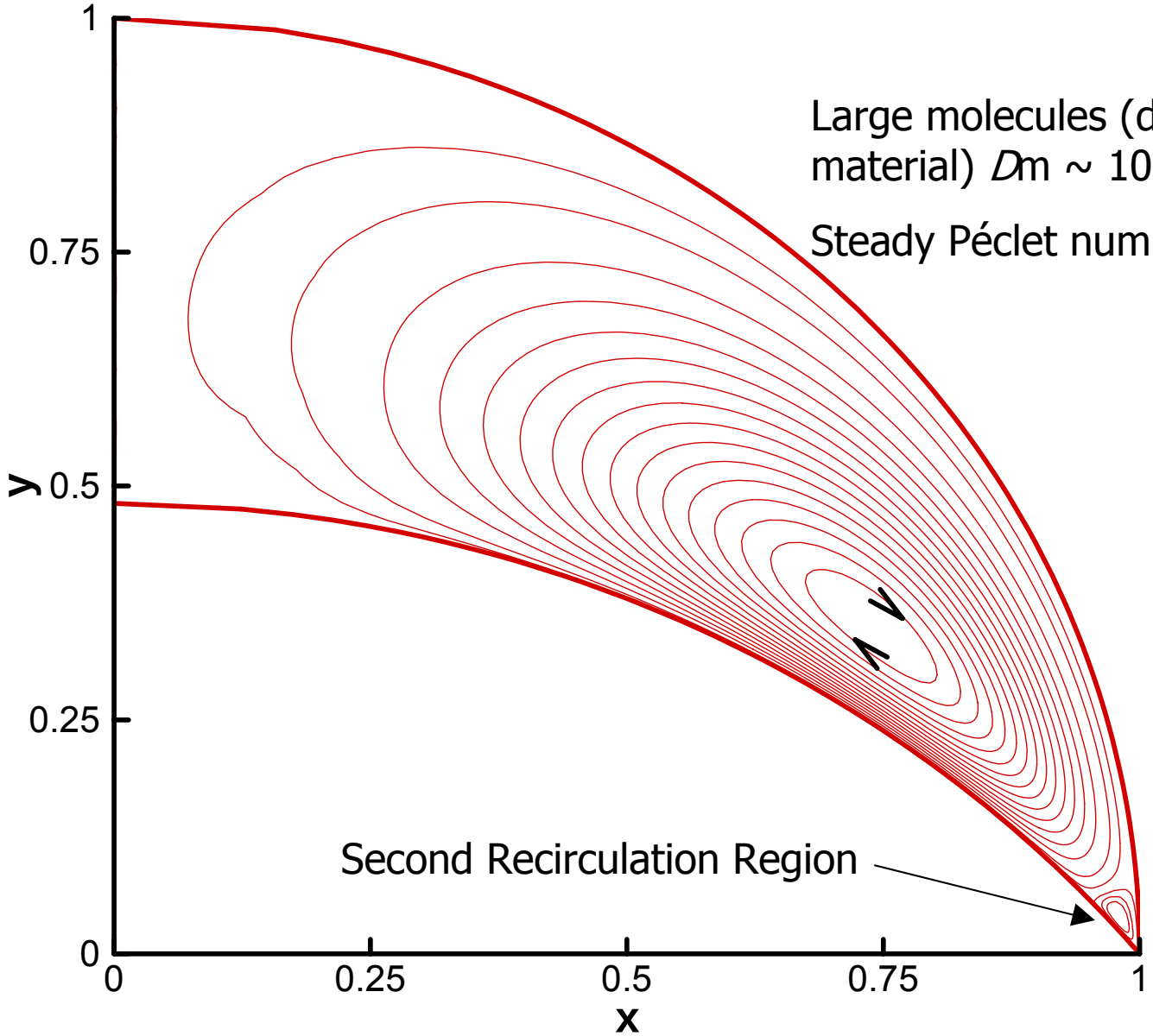

Large molecules (drugs, genetic material) $D_m \sim 10^{-8}$ cm^2/s)

Steady Péclet number O(1) to O(10^2)

V=0.9, Δ=0.2, $\alpha=\pi/2$, Ma=4.0, Ps=10.0, K=0.5

Cycle-Averaged Streamlines – K=0.7

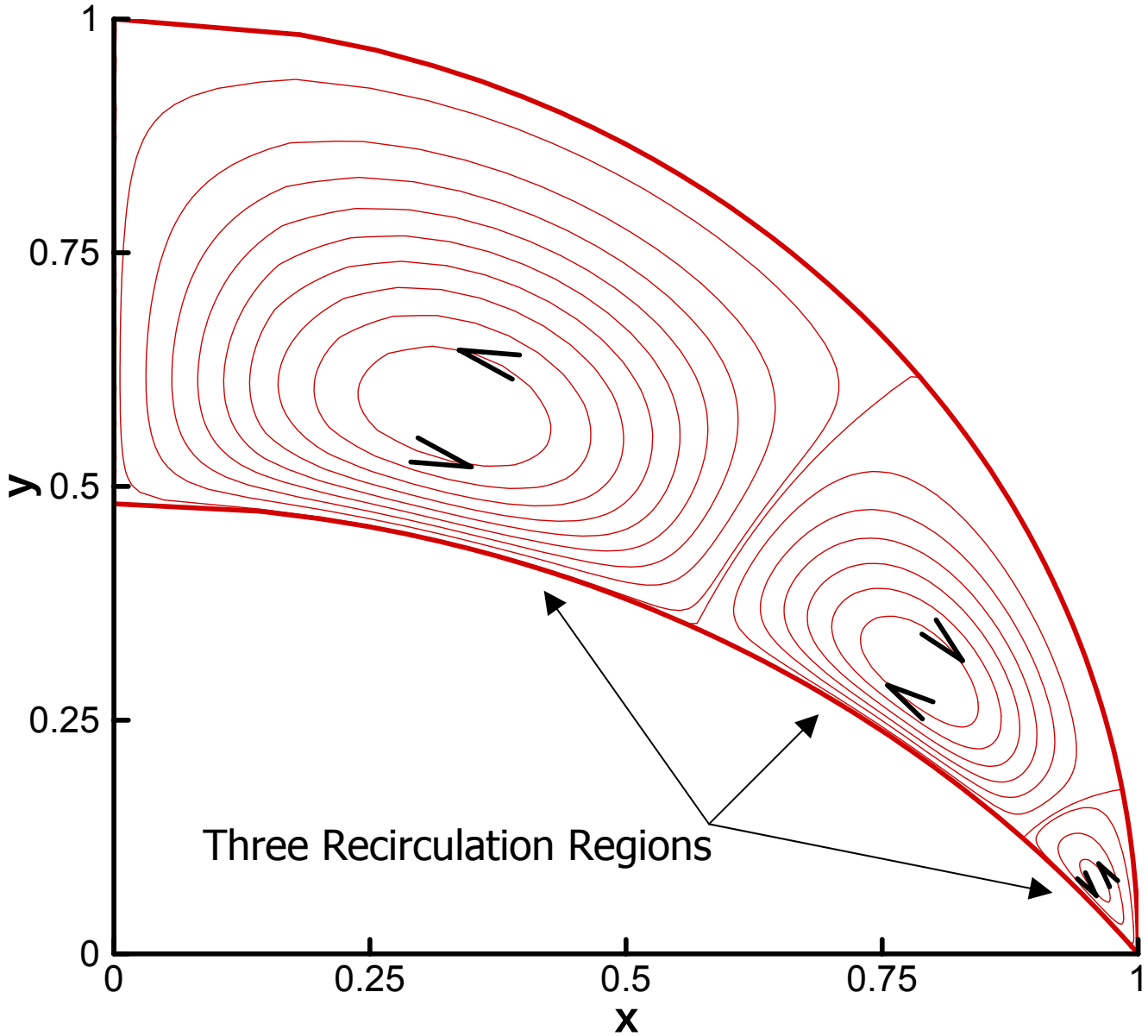

V=0.9, Δ=0.2, $\alpha=\pi/2$, Ma=4.0, Ps=10.0,K=0.7

Cycle-Averaged Streamlines – K=1.0

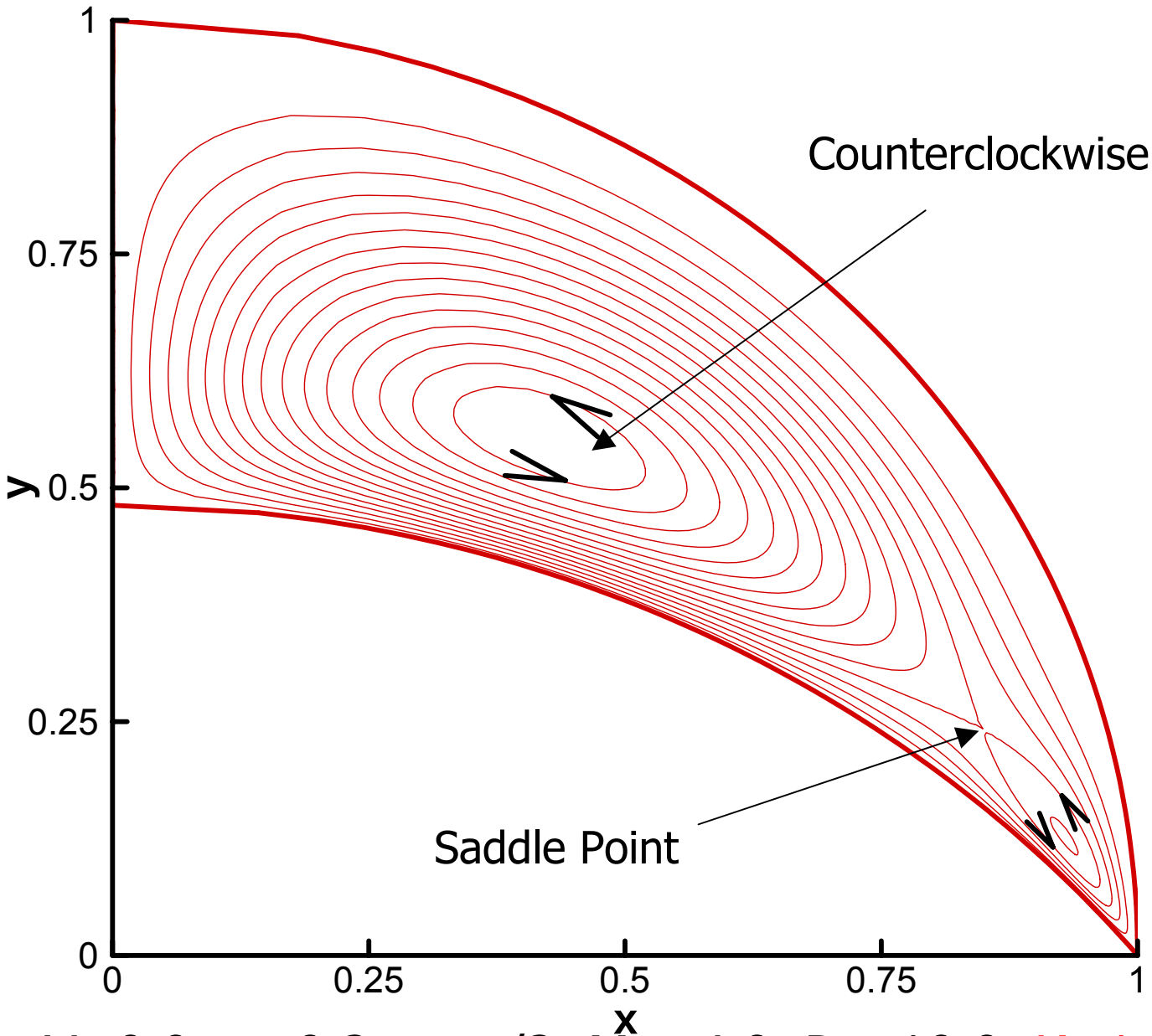

V=0.9, Δ=0.2, α=π/2, Ma=4.0, Ps=10.0, K=1.0

Models of Airway Closure: Effects of Tube Elasticity, Surfactants, and Oscillatory Core Flow

James B. Grotberg[1] & David Halpern[2]

[1]Department of Biomedical Engineering
University of Michigan
Ann Arbor, MI

[2]Department of Mathematics
University of Alabama
Tuscaloosa, AL

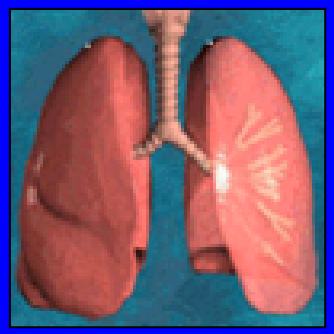

Effects of Flexibility and Surfactant on Airway Closure

Halpern & Grotberg, JBE 1993

Fluid: $\frac{\partial h}{\partial t}=\frac{1}{1+\epsilon(h-1)}\left[(1+\epsilon\eta)\frac{\partial \eta}{\partial t}+\frac{\partial Q_w}{\partial z}\right]$ $\quad Q_w=\int_0^Y w dy=-\frac{Y^3}{3}\frac{\partial p}{\partial z}+\frac{Y^2}{2}\frac{\partial \bar{\sigma}}{\partial z}$

Elastic Tube: $\phi\frac{\partial \eta}{\partial t}-T_l\frac{\partial^2 \eta}{\partial z^2}+\frac{1}{\Gamma}\frac{\eta}{(1+\epsilon\eta)^2}=\frac{\partial^2 h}{\partial z^2}+\frac{h}{(1-\epsilon)(1+\epsilon(h-1))^3}$

Insoluble Surfactant: $\frac{\partial \bar{C}}{\partial t}=\frac{1}{Pe_s}\frac{\partial^2 \bar{C}}{\partial z^2}-\frac{1}{\epsilon^2}\frac{\partial}{\partial z}(w_s(1+\epsilon^2\bar{C}))$

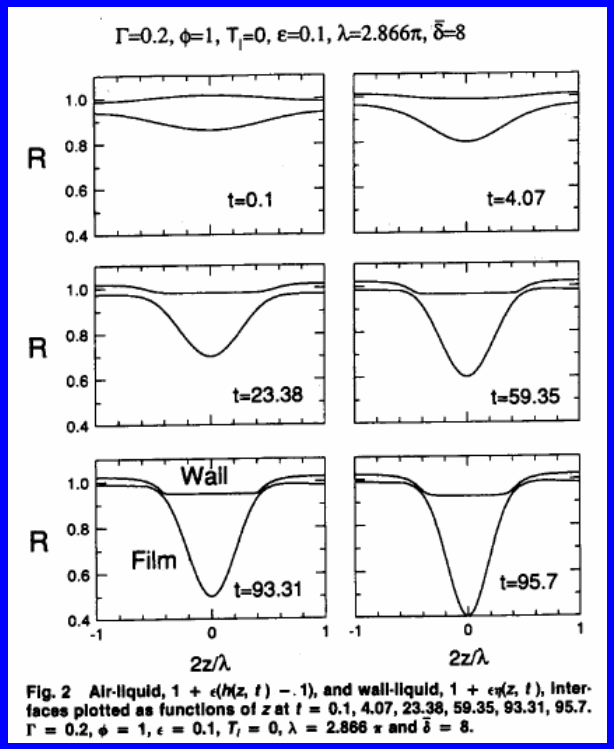

Fig. 2 Air-liquid, $1+\epsilon(h(z,t)-1)$, and wall-liquid, $1+\epsilon\eta(z,t)$, interfaces plotted as functions of z at t = 0.1, 4.07, 23.38, 59.35, 93.31, 95.7. Γ = 0.2, ϕ = 1, ϵ = 0.1, T_l = 0, λ = 2.866 π and $\bar{\delta}$ = 8.

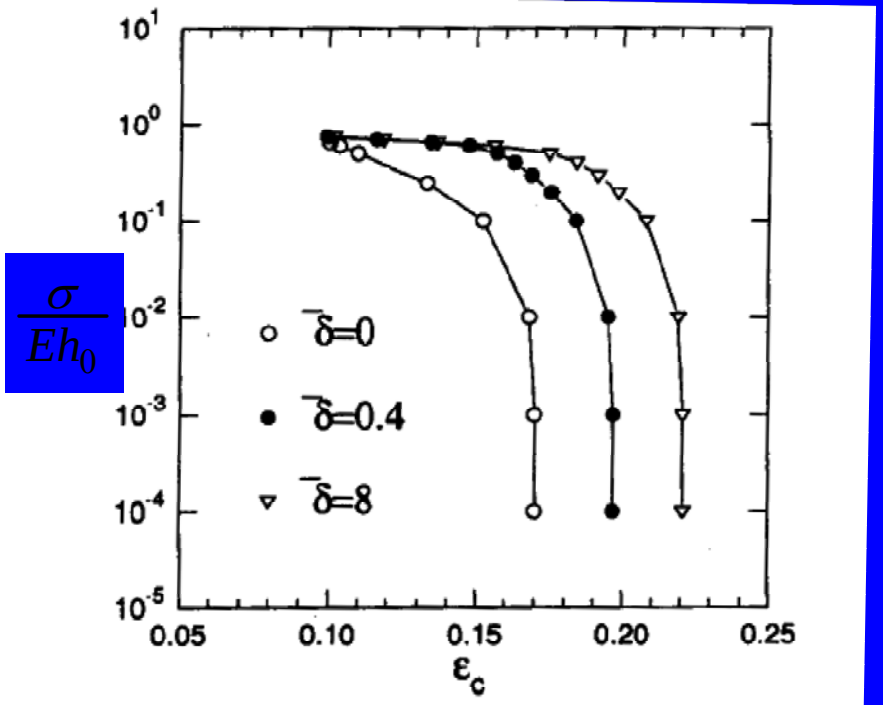

Fig. 6 Γ versus ϵ_c for $\phi = 5 \times 10^{-4}$, T_l = 1.25, λ = 6, $\bar{\delta}$ = 0, 0.4, 8.

Airway Closure in Normal Gravity

- Occurs in lower lung only
- Local atelectesis
- Regional ventilation inhomogeneity
- Mismatch of ventilation and perfusion

Airway Closure in Microgravity

- Can occur everywhere

Effects of Oscillatory Core Flow in a Liquid-Lined Rigid Tube

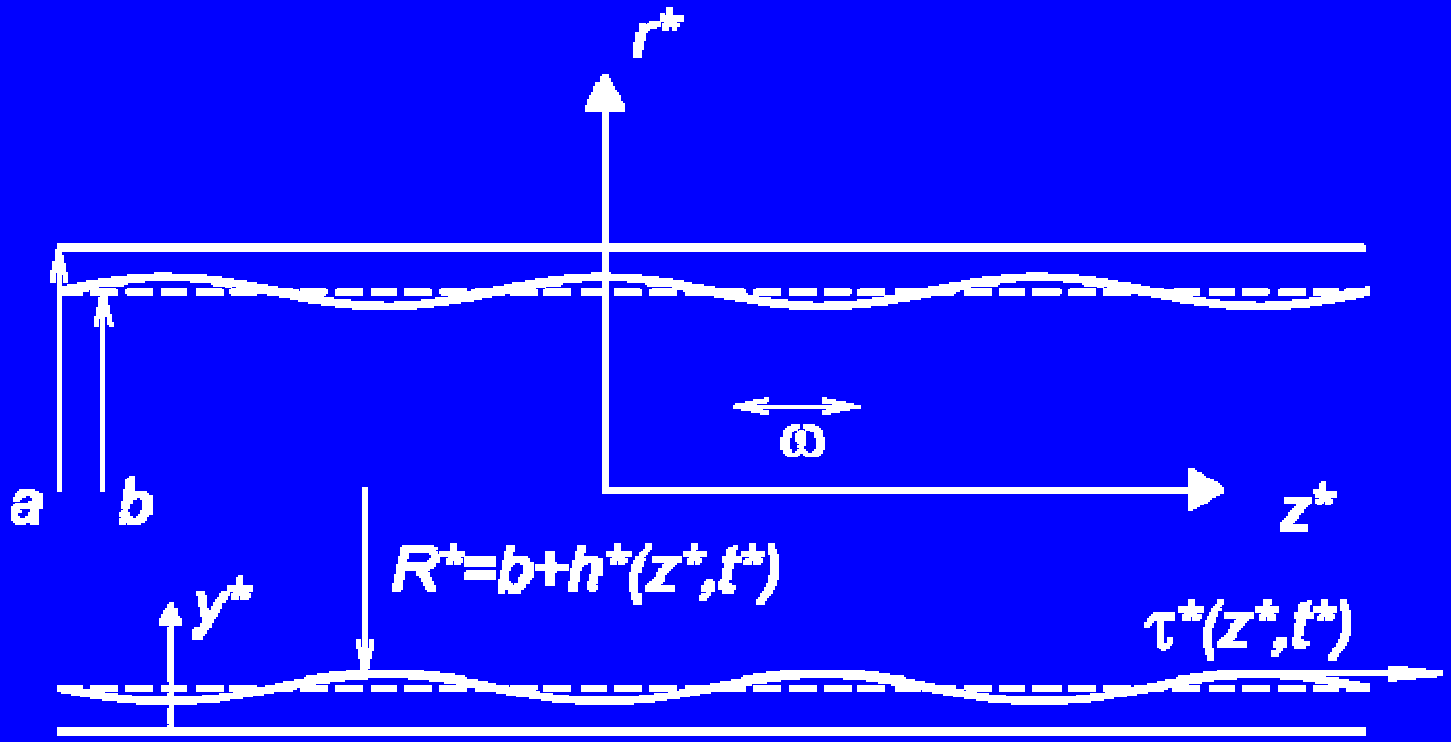

Parameters: $\lambda = V_T / \pi b^3$ $\Omega = \omega a / (\varepsilon^3 \sigma / \mu_f)$

$$\varepsilon = \frac{a-b}{a}, \ \alpha^2 = \omega b^2 / \upsilon_c, \ Ca = \mu_c \omega L_T / \varepsilon^2 \sigma$$

Model Assumptions

1. Film consists of incompressible Newtonian fluid
2. Oscillatory core flow provides shear-stress at interface
3. Flow in thin film governed by lubrication theory
4. Low-viscosity core fluid perceives the thin, high-viscosity film as a rigid boundary, uncoupled problem
5. Interface deformation is quasi-steady with respect to the core fluid motion
6. Long wave approximation
7. Fixed tidal volume

Unperturbed Closure

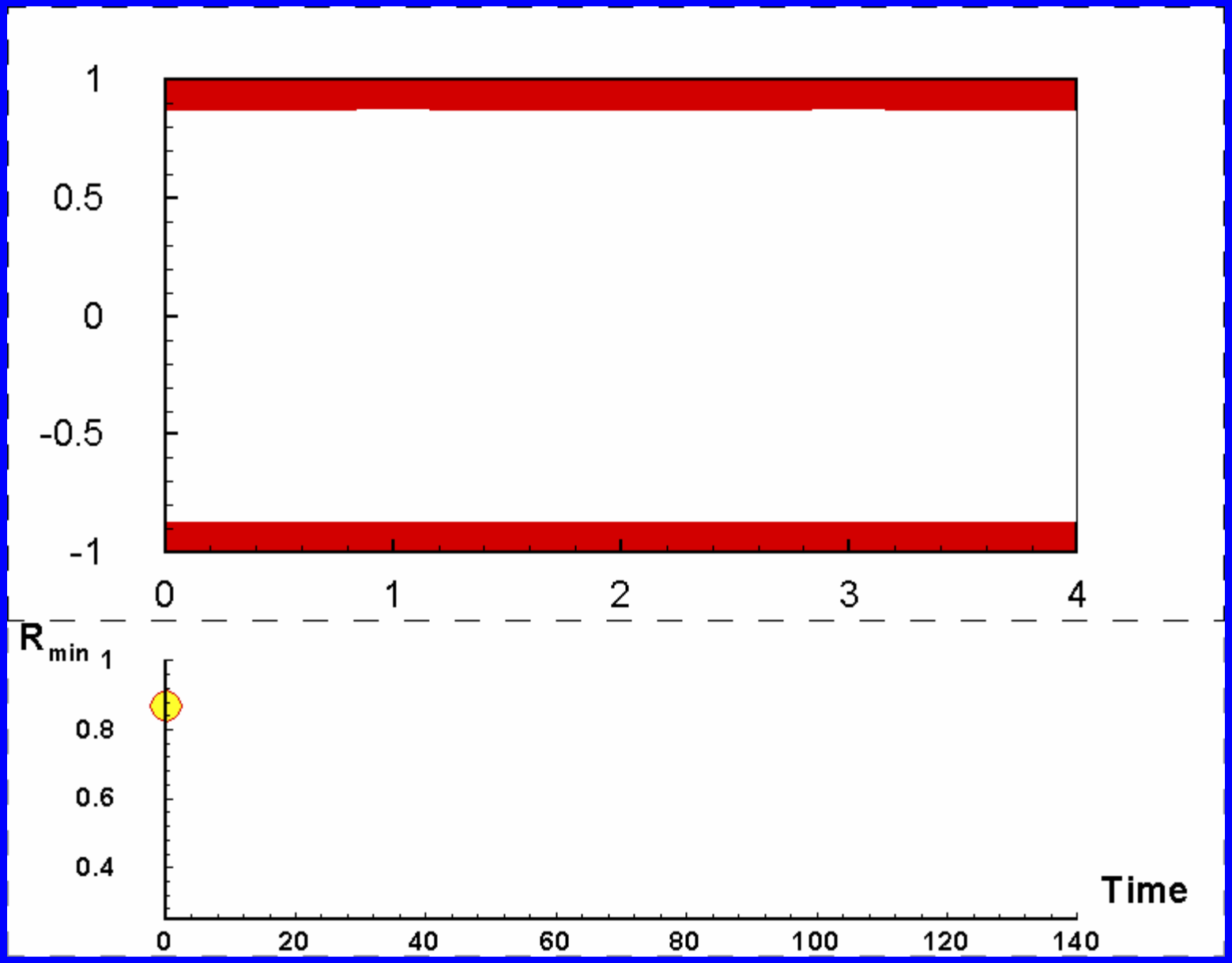

Oscillatory Core Flow

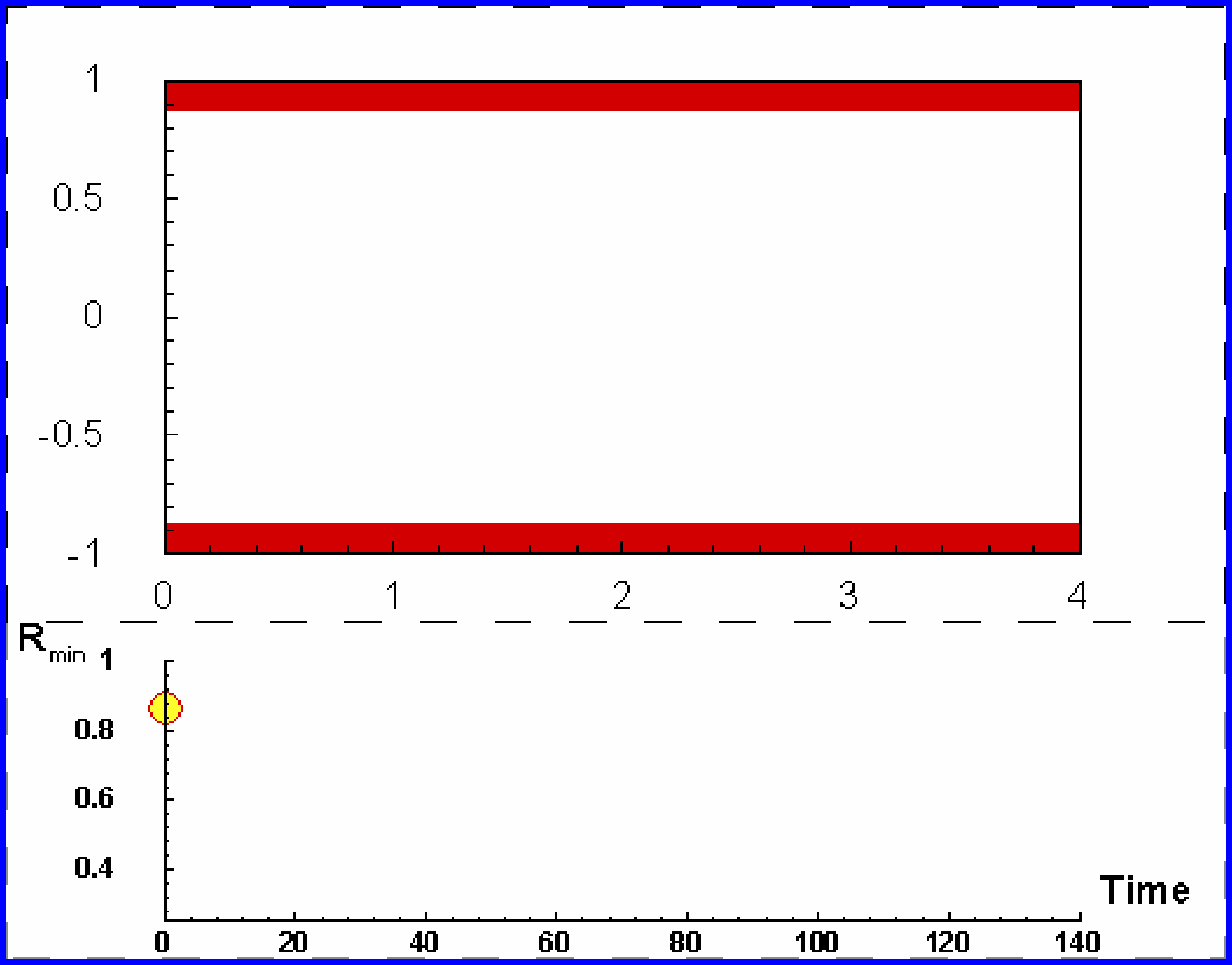

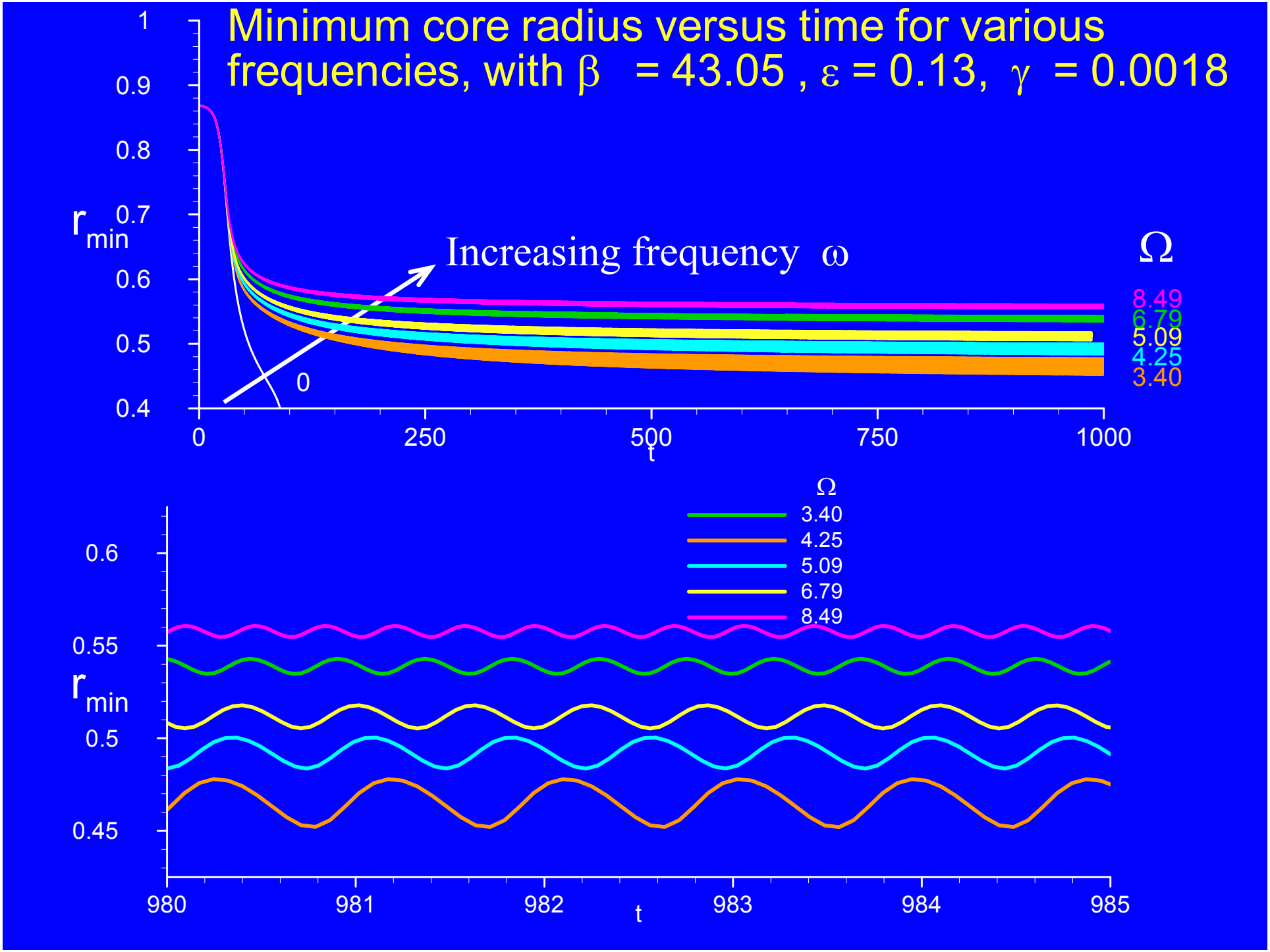
Minimum core radius versus time for various frequencies, with β = 43.05 , ε = 0.13, γ = 0.0018
r min
1
0.9
0.8
0.7
0.6
0.5
0.4
0
250
500
750
1000
t
Increasing frequency ω
0
Ω
8.49
6.79
5.09
4.25
3.40
Ω
3.40
4.25
5.09
6.79
8.49
r min
0.6
0.55
0.5
0.45
980
981
982
983
984
985
t

Mechanism "Reversing Butter Knife"

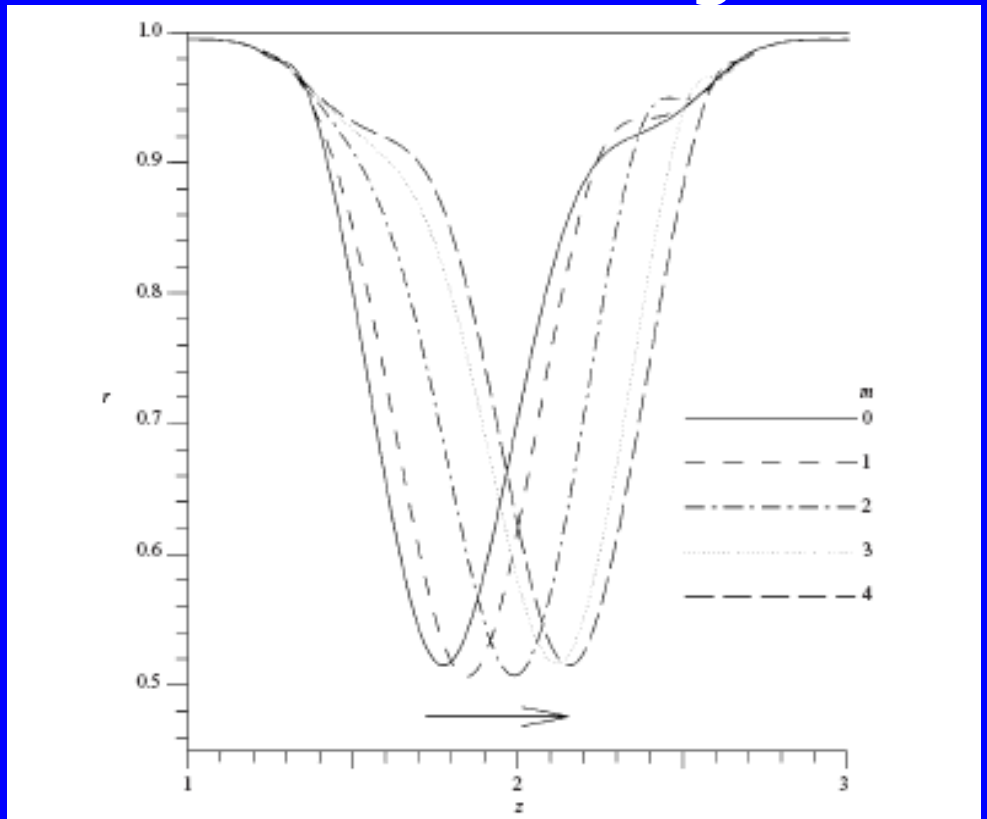

FIGURE 6. The shape of the airway–liquid interface, $1-\varepsilon+\varepsilon h(z,t)$ at $t=t_0+\varkappa m/4\Omega$, where $t_0=986.7228$, $\Omega=5.094$, $\varepsilon=0.13$, $\lambda=14.86$ and $0\leqslant m\leqslant 4$.

During stroke: trailing film thicker than leading film → bulge diminishes

During turn around: capillary instability → bulge grows

Needs tuning with high enough frequency

Students, Grand-Students, Great-Grand-Students….

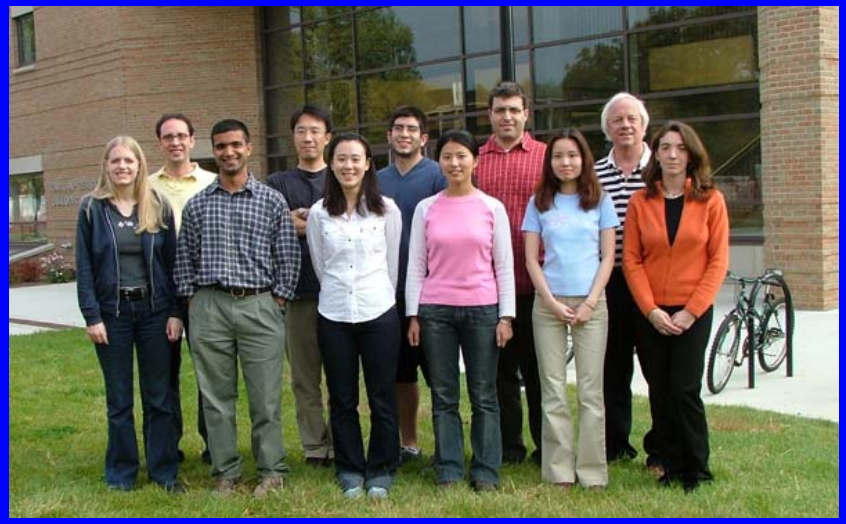

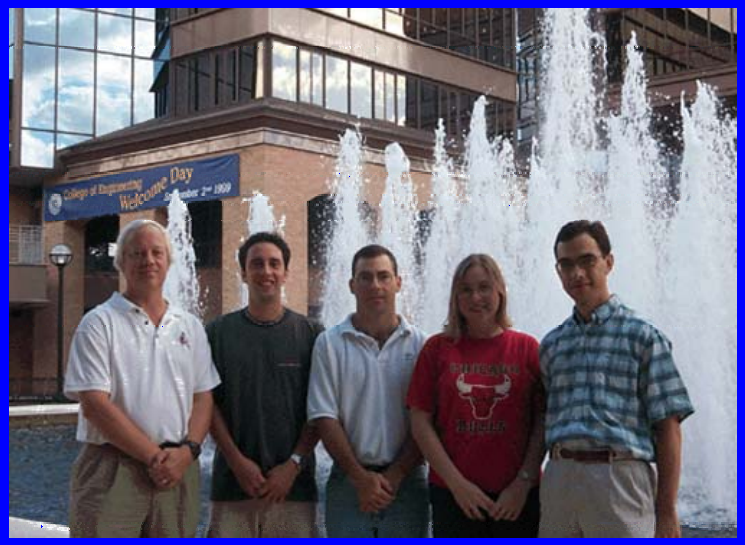

NSF, NIH, NASA, Whitaker Foundation